Weierstraß-Institut
für Angewandte Analysis und Stochastik
Leibniz-Institut im Forschungsverbund Berlin e. V.

Preprint ISSN 0946 – 8633

MAC schemes on triangular Delaunay meshes

Robert Eymard[1], Jürgen Fuhrmann [2], Alexander Linke[2]

[1] Université Paris-Est Marne La Vallée
5, boulevard Descartes
Champs-sur-Marne
77454 Marne La Vallée CEDEX 2
France
robert.eymard@univ-mlv.fr

[2] Weierstrass Institute
Mohrenstr. 39
10117 Berlin
Germany
juergen.fuhrmann@wias-berlin.de
alexander.linke@wias-berlin.de

submitted: October 18, 2011

No. 1654
Berlin 2011

2010 *Mathematics Subject Classification.* 76D05,65N08.

Key words and phrases. incompressible Navier-Stokes equations, generalized MAC discretization, unstructured Delaunay grid, finite volume method, coupled flow problem, convergence proof.

Edited by
Weierstraß-Institut für Angewandte Analysis und Stochastik (WIAS)
Leibniz-Institut im Forschungsverbund Berlin e. V.
Mohrenstraße 39
10117 Berlin
Germany

Fax: +49 30 2044975
E-Mail: preprint@wias-berlin.de
World Wide Web: http://www.wias-berlin.de/

Abstract. We study two classical generalized MAC schemes on unstructured triangular Delaunay meshes for the incompressible Stokes and Navier-Stokes equations and prove their convergence for the first time. These generalizations use the duality between Voronoi boxes and triangles of Delaunay meshes, in order to construct two staggered discretization schemes. Both schemes are especially interesting in coupled flow problems, since compatible finite volume discretizations for coupled convection-diffusion equations can be constructed which preserve discrete maximum principles. In the first scheme, called tangential velocity scheme, the pressures are defined at the vertices of the mesh, and the discrete velocities are tangential to the edges of the triangles. In the second scheme, called normal velocity scheme, the pressures are defined in the triangles, and the discrete velocities are normal to the edges of the triangles. For both schemes, we prove the strong convergence in L^2 for the velocities and the discrete rotations of the velocities for the Stokes and the Navier-Stokes problem. Further, for the normal velocity scheme we also prove the strong convergence of the pressure in L^2. Linear and nonlinear numerical examples illustrate the theoretical predictions.

1. Introduction

We consider in this paper two different generalizations [**2, 14, 17, 13, 20**] of the classical MAC scheme [**15, 21**] for the incompressible Stokes and Navier-Stokes equations in two space dimensions and prove their convergence for the first time. In the Stokes problem, we look for the unique weak solution $(\boldsymbol{v}, p) \in H_0^1(\Omega)^2 \times L^2(\Omega)$ of the system

$$-\Delta \boldsymbol{v} + \nabla p = \boldsymbol{f} \qquad \boldsymbol{x} \in \Omega, \tag{1.1}$$

$$\nabla \cdot \boldsymbol{v} = 0 \qquad \boldsymbol{x} \in \Omega, \tag{1.2}$$

$$\int_\Omega p \, \mathrm{d}\boldsymbol{x} = 0 \tag{1.3}$$

$$\boldsymbol{v} = 0 \qquad \boldsymbol{x} \in \partial\Omega, \tag{1.4}$$

where $\boldsymbol{f}$ is assumed to be in $L^2(\Omega)^2$. In the nonlinear case, we investigate the Navier-Stokes equations in the so-called rotation form, where we have to use the Bernoulli pressure $P = p + \frac{1}{2}\boldsymbol{v}^2$. Then, these equations read

$$-\Delta \boldsymbol{v} + (\operatorname{rot} \boldsymbol{v})\, \boldsymbol{v}^\perp + \nabla P = \boldsymbol{f} \qquad \boldsymbol{x} \in \Omega,$$

$$\nabla \cdot \boldsymbol{v} = 0 \qquad \boldsymbol{x} \in \Omega,$$

$$\int_\Omega P \, \mathrm{d}\boldsymbol{x} = 0$$

$$\boldsymbol{v} = 0 \qquad \boldsymbol{x} \in \partial\Omega,$$

where $(v_1, v_2)^\perp$ is defined as $(-v_2, v_1)$. We assume that the following hypotheses are fulfilled:

$$\Omega \subset \mathbb{R}^2 \text{ is an polygonal bounded and connected domain without holes,}$$

$$\text{with the boundary } \partial\Omega, \tag{1.5}$$

$$\boldsymbol{f} \in L^2(\Omega)^2. \tag{1.6}$$

Numerous discretization schemes have been developed in the recent past for the approximation of the incompressible Stokes and Navier-Stokes equations. Among them, the classical MAC scheme [**15, 21**] is one of the best-known. It is based on a staggered approach on structured grids, where the velocity and the pressure control volumes are dual to each other and have square or rectangular shape. Since the scheme is staggered, the pressure is not prone to instabilities. In this situation, convergence proofs for the linear Stokes and the nonlinear Navier–Stokes problems (with small data assumption) have been presented by Nicolaides and coauthors [**20, 18, 19**]. But in spite of its success, this scheme has the main drawback that complex geometries cannot be well approximated by rectangular grids. Therefore, several attempts have been made to generalize it for unstructured grids, see e.g., [**16, 2, 14, 17, 13, 20**]. While the extension by Kanschat [**16**] is in the spirit of discontinuous Galerkin methods, the extensions given in Refs. [**2, 14, 17, 13, 20**] are more in the spirit of finite volume methods where the unstructured simplex grid possesses the Delaunay property. Then the dual

Voronoi grid can be defined in a simple geometrical way (see Figure 1), and two different staggered approaches are possible:

(1) in the first scheme, called the *tangential velocity scheme*, the velocity is approximated by its tangential values along the edges of the triangles, whereas the pressures are approximated at the vertices of the triangles;
(2) in the second scheme, called the *normal velocity scheme*, the velocity is approximated by its normal values to the edges of the triangles, whereas the pressures are approximated at the center of the triangles.

These generalized MAC schemes on Delaunay-Voronoi meshes are especially interesting for coupled flow problems. For the tangential velocity scheme, the proposed discretization of $\nabla \cdot \boldsymbol{u} = 0$ exactly coincides with the discrete solenoidal condition allowing to prove a discrete maximum principle for the Voronoi finite volume method for convective transport of a dissolved species in the velocity field $\boldsymbol{u}$ [**9, 10**]. Hence it is particularly interesting to study the convergence of these schemes.

Let us notice that the convergence proofs for the MAC scheme have been given by Nicolaides and his coauthors for the case of rectangular meshes and may not easily be extended to general triangular meshes. Indeed, in the case of the tangential velocity scheme, a consistent discrete rotation operator is obtained if the discrete velocity degrees of freedom are located at the midpoint of the triangle edges, but a consistent divergence operator demands that the discrete velocity degrees of freedom are at the midpoint of the Voronoi edges (see Figure 1, which shows that these two points are different in the general case).

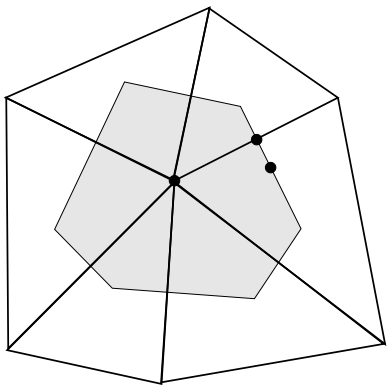

FIGURE 1. Triangular and Voronoi meshes, midpoints of triangle edges and Voronoi edges.

In the case of the normal velocity scheme, the points used for the definition of the discrete rotation and divergence are exchanged in comparison to the tangential scheme. It results that for both schemes, the discrete divergence and discrete rotation operators cannot be simultaneously consistent, and standard convergence proofs based on error estimates fail. In order to overcome this difficulty, we apply discrete Helmholtz decompositions which lead to the study of two nonconforming discrete schemes for the biharmonic problem. The convergence of these schemes has been proven in two recent papers [**6, 7**], yielding the convergence of the velocity / pressure schemes to the continuous weak formulation of the Stokes problem.

The main results of the paper are the following: For both schemes, we show the strong convergence in L^2 of some reconstructions of the velocities, and we prove the strong convergence of their discrete rotation in L^2. We only prove the convergence of the pressure (in L^2) in the case of the normal velocity scheme, which allows a simple discrete Nečas lifting. After that, using a strong reconstruction of the velocity, we prove the convergence of the corresponding schemes for the Navier-Stokes equation in the Bernoulli pressure formulation. Finally, numerical results for both schemes are presented at the end of the paper. Remark that they also show the numerical convergence of the pressure for the tangential velocity scheme.

2. Definition of the schemes

DEFINITION 2.1 (Acute triangular mesh of Ω). Under hypothesis (1.5), an acute triangular mesh of the domain Ω is defined by $\mathcal{M} = (\mathcal{V}, \mathcal{E}, \mathcal{T})$, such that:

(1) The set $\mathcal{T}$ is the finite set of disjoint triangles (considered as open subsets of $\mathbb{R}^2$) such that $\bigcup_{T\in\mathcal{T}} \overline{T} = \overline{\Omega}$. We denote by $h_{\mathcal{M}}$ the largest diameter of all triangles. For all $T \in \mathcal{T}$, the point $\boldsymbol{x}_T$, defined as the center of the circumcircle of T, is such that $\boldsymbol{x}_T \in T$.
(2) The set $\mathcal{V}$ consists of the vertices of all the triangles. For all $\boldsymbol{y} \in \mathcal{V}$, we denote by $V_{\boldsymbol{y}}$ the Voronoi box around the vertex $\boldsymbol{y} \in \mathcal{V}$, defined as $V_{\boldsymbol{y}} = \{\boldsymbol{x} \in \Omega, |\boldsymbol{x} - \boldsymbol{y}| < |\boldsymbol{x} - \boldsymbol{y'}| \text{ for all } \boldsymbol{y'} \in \mathcal{V}, \boldsymbol{y'} \neq \boldsymbol{y}\}$.
(3) The set $\mathcal{E}$ consists of all the edges of the triangles, and is such that, for all $\sigma \in \mathcal{E}$, either σ is located on the boundary of Ω (we denote by $\mathcal{E}_{\text{bnd}}$ the set of these boundary edges), or σ is common to two neighboring triangles (we denote by $\mathcal{E}_{\text{int}}$ the set of these interior edges). We then denote by $\boldsymbol{x}_\sigma$ the midpoint of σ and by $\theta_{\mathcal{M}}$ the infimum of all quantities $|\boldsymbol{x}_\sigma - \boldsymbol{x}_T|/h_T$, for all triangles T, and $h_T/h_{T'}$, for any pair of neighbouring triangles T and T'.

REMARK 2.2. The acuteness assumption which is equivalent to the conditioon that the circumcenters $\boldsymbol{x}_T$ of all triangles $T \in \mathcal{T}$ are inside their triangles can be weakened. We are convinced that it would be sufficient that the triangulation is *boundary conforming Delaunay* [**25**], which means that it is Delaunay, and all triangle circumcenters are contained in the domain Ω. In fact, we will use such meshes for our numerical computations. For the sake of simplicity in the proofs, we restrict our theoretical results to acute meshes.

For every edge $\sigma \in \mathcal{E}$, we define a fixed orientation, which is given by an unit vector $\boldsymbol{t}_\sigma$ parallel to σ, and we define $\boldsymbol{n}_\sigma$ as the normal vector to σ, obtained from $\boldsymbol{t}_\sigma$ by a rotation with angle $\pi/2$ in the counterclockwise sense (this rotation operator will be denoted as $\rho_{\frac{\pi}{2}}$, see Figure 2). We further assume that the edges $\sigma \in \mathcal{E}_{\text{bnd}}$ at the border of Ω build a counterclockwise path around Ω. Then, for any edge $\sigma \in \mathcal{E}_{\text{bnd}}$, the exterior of Ω is located to the right of σ.

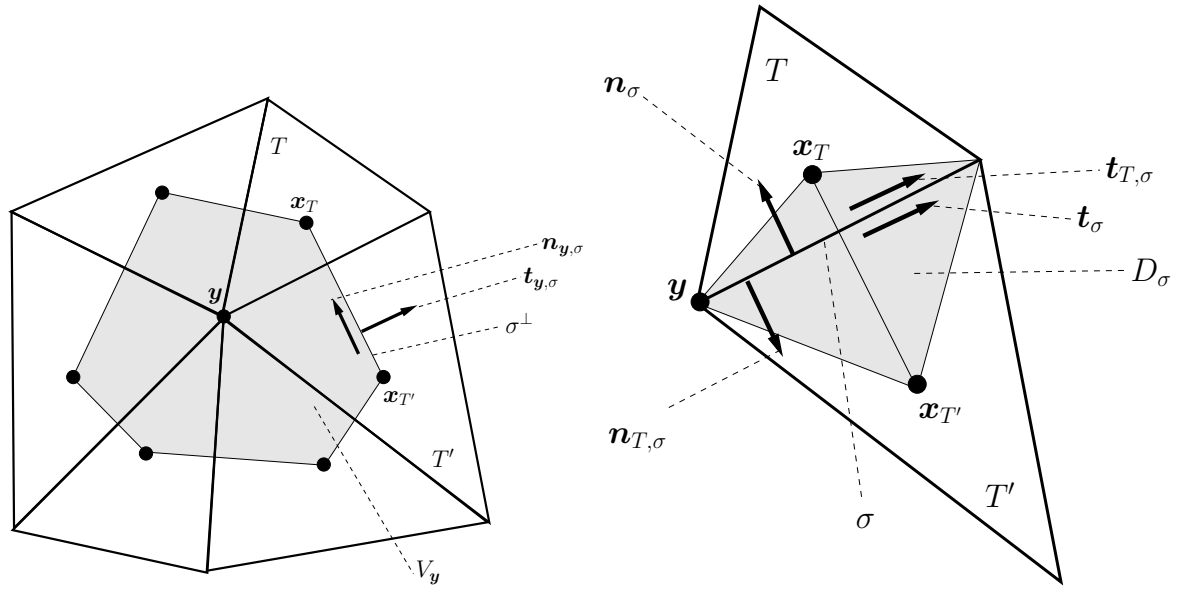

FIGURE 2. Notations for the mesh: Left: the Voronoi box associated to a vertex. Right: Zoom into a diamond.

For every $T \in \mathcal{T}$, we denote by $\mathcal{E}_T$ the set of edges of the triangle T, and we denote, for any $\sigma \in \mathcal{E}_T$, by $\boldsymbol{t}_{T,\sigma}$ the unit vector parallel to σ oriented in the counterclockwise sense around T, by $\boldsymbol{n}_{T,\sigma}$ the unit vector normal to σ and outward to T, and by $D_{T,\sigma}$ the cone with basis σ and vertex $\boldsymbol{x}_T$.

For any $\sigma \in \mathcal{E}_{\text{int}}$, let T and T' be the two neighboring triangles such that σ is an edge of T and T'. We denote by $\sigma^\perp$ the segment (Voronoi face) $[\boldsymbol{x}_T, \boldsymbol{x}_{T'}]$, by $\boldsymbol{x}_{\sigma^\perp} = \frac{1}{2}(\boldsymbol{x}_T + \boldsymbol{x}_{T'})$ the midpoint of the Voronoi face $\sigma^\perp$, and by $D_\sigma = D_{T,\sigma} \cup D_{T',\sigma}$. For any $\sigma \in \mathcal{E}_{\text{bnd}}$, let T be the triangle such that σ is an edge of T. We then denote by $\sigma^\perp$ the segment $[\boldsymbol{x}_T, \boldsymbol{x}_\sigma]$ and by $D_\sigma = D_{T,\sigma}$.

For any $\boldsymbol{y} \in \mathcal{V}$, we denote by $\mathcal{E}_{\boldsymbol{y}}$ the set of all the edges which have $\boldsymbol{y}$ as a vertex, and we denote, for any $\sigma \in \mathcal{E}_{\boldsymbol{y}}$, by $\boldsymbol{t}_{\boldsymbol{y},\sigma}$ the unit vector parallel to σ oriented from $\boldsymbol{y}$ to the other vertex of σ and by $\boldsymbol{n}_{\boldsymbol{y},\sigma}$ the unit vector normal to σ and in the counterclockwise sense around $\boldsymbol{y}$.

DEFINITION 2.3. By curl: $H^1(\Omega) \to L^2(\Omega)^2$ and rot: $H^1(\Omega)^2 \to L^2(\Omega)$ we denote the following two differential operators

$$\operatorname{curl} \xi = \begin{pmatrix} \partial_y \xi \\ -\partial_x \xi \end{pmatrix} \qquad \forall \xi \in H^1(\Omega),$$

and

$$\operatorname{rot} \begin{pmatrix} p \\ q \end{pmatrix} = \partial_x q - \partial_y p \qquad \forall p, q \in H^1(\Omega).$$

Note that $\operatorname{rot} \operatorname{curl} \xi = -\Delta \xi$ holds for all $\xi \in H^2(\Omega)$.

2.1. Tangential velocity scheme. Let us now define the tangential velocity scheme, where the space of degrees of freedom for the velocities and the pressures will be respectively denoted by

$$X_{\mathcal{E}} = \mathbb{R}^{\mathcal{E}}, \tag{2.1}$$

$$X_{\mathcal{V}} = \mathbb{R}^{\mathcal{V}}. \tag{2.2}$$

The degrees of freedom for the velocity represent the velocity components $\boldsymbol{v} \cdot \boldsymbol{t}_\sigma$ at the midpoint of the edges $\sigma \in \mathcal{E}$, which are oriented in the direction $\boldsymbol{t}_\sigma$. The degrees of freedom for the pressure represent the pressure at the vertices of the triangulation. The space

$$\dot{X}_{\mathcal{E}} = \{v \in X_{\mathcal{E}}, v_\sigma = 0, \forall \sigma \in \mathcal{E}_{\text{ext}}\} \tag{2.3}$$

represents the degrees of freedom for the velocity, when homogeneous Dirichlet boundary conditions are prescribed at the boundary edges.

Let us introduce the discrete differential operators which are needed for the tangential velocity scheme

$$\operatorname{rot}_T v = \frac{1}{|T|} \sum_{\sigma \in \mathcal{E}_T} |\sigma| v_\sigma \boldsymbol{t}_\sigma \cdot \boldsymbol{t}_{T,\sigma} \qquad \forall v \in X_{\mathcal{E}},\ \forall T \in \mathcal{T}, \tag{2.4}$$

$$\operatorname{div}_{\boldsymbol{y}} v = \frac{1}{|V_{\boldsymbol{y}}|} \sum_{\sigma \in \mathcal{E}_{\boldsymbol{y}}} |\sigma^\perp| v_\sigma \boldsymbol{t}_\sigma \cdot \boldsymbol{t}_{\boldsymbol{y},\sigma} \qquad \forall v \in X_{\mathcal{E}},\ \forall \boldsymbol{y} \in \mathcal{V}, \tag{2.5}$$

see Figure 2 for the notations used here. Then the scheme reads:

find $(v, p_{\mathcal{V}}) \in \dot{X}_{\mathcal{E}} \times X_{\mathcal{V}}$ such that

$$\sum_{T \in \mathcal{T}} |T| \operatorname{rot}_T v \operatorname{rot}_T w - \sum_{\boldsymbol{y} \in \mathcal{V}} |V_{\boldsymbol{y}}| p_{\boldsymbol{y}} \operatorname{div}_{\boldsymbol{y}} w = \sum_{\sigma \in \mathcal{E}} 2 w_\sigma \int_{D_\sigma} \boldsymbol{f} \cdot \boldsymbol{t}_\sigma \mathrm{d}\boldsymbol{x},\ \forall w \in \dot{X}_{\mathcal{E}} \tag{2.6}$$

$$\sum_{\boldsymbol{y} \in \mathcal{V}} |V_{\boldsymbol{y}}| p_{\boldsymbol{y}} = 0, \tag{2.7}$$

$$\operatorname{div}_{\boldsymbol{y}} v = 0,\ \forall \boldsymbol{y} \in \mathcal{V}. \tag{2.8}$$

It is possible to write the above scheme, using functions defined on the spatial domain Ω by

$$\operatorname{rot}_{\mathcal{T}} v(\boldsymbol{x}) = \operatorname{rot}_T v \qquad \forall v \in X_{\mathcal{E}},\ \forall T \in \mathcal{T}, \text{for a.e. } \boldsymbol{x} \in T, \tag{2.9}$$

$$\operatorname{div}_{\mathcal{V}} v(\boldsymbol{x}) = \operatorname{div}_{\boldsymbol{y}} v \qquad \forall v \in X_{\mathcal{E}}, \forall \boldsymbol{y} \in \mathcal{V}, \text{for a.e. } \boldsymbol{x} \in V_{\boldsymbol{y}}, \tag{2.10}$$

$$\mathcal{R}_{\mathcal{E}}^{\parallel} w(\boldsymbol{x}) = 2 w_\sigma \boldsymbol{t}_\sigma \qquad \forall w \in X_{\mathcal{E}},\ \forall \sigma \in \mathcal{E},\ \text{for a.e. } \boldsymbol{x} \in D_\sigma, \tag{2.11}$$

$$\mathcal{R}_{\mathcal{V}} p_{\mathcal{V}}(\boldsymbol{x}) = p_{\boldsymbol{y}} \qquad \forall p \in X_{\mathcal{V}},\ \forall \boldsymbol{y} \in \mathcal{V}, \text{for a.e. } \boldsymbol{x} \in V_{\boldsymbol{y}}. \tag{2.12}$$

We can then rewrite (2.6)-(2.7)-(2.8) in the following way:

find $(v, p_{\mathcal{V}}) \in \dot{X}_{\mathcal{E}} \times X_{\mathcal{V}}$ such that

$$\int_\Omega \operatorname{rot}_{\mathcal{T}} v(\boldsymbol{x}) \operatorname{rot}_{\mathcal{T}} w(\boldsymbol{x}) \mathrm{d}\boldsymbol{x} - \int_\Omega \mathcal{R}_{\mathcal{V}} p_{\mathcal{V}}(\boldsymbol{x}) \operatorname{div}_{\mathcal{V}} w(\boldsymbol{x}) \mathrm{d}\boldsymbol{x} = \int_\Omega \boldsymbol{f}(\boldsymbol{x}) \cdot \mathcal{R}_{\mathcal{E}}^{\parallel} w(\boldsymbol{x}) \mathrm{d}\boldsymbol{x},\ \forall w \in \dot{X}_{\mathcal{E}}, \tag{2.13}$$

$$\int_\Omega \mathcal{R}_{\mathcal{V}} p_{\mathcal{V}}(\boldsymbol{x}) \mathrm{d}\boldsymbol{x} = 0, \tag{2.14}$$

$$\operatorname{div}_{\mathcal{V}} v(\boldsymbol{x}) = 0 \text{ for a.e. } \boldsymbol{x} \in \Omega. \tag{2.15}$$

Further, it is possible to write Problem (2.13)-(2.14)-(2.15) without using the pressure. We denote by

$$V_{\mathcal{E}}^{\parallel} = \{v \in \dot{X}_{\mathcal{E}}, \operatorname{div}_{\mathcal{V}} v = 0\}. \tag{2.16}$$

We then notice that a solution of Problem (2.13)-(2.14)-(2.15) also satisfies

$$v \in V_{\mathcal{E}}^{\parallel}, \int_{\Omega} \operatorname{rot}_{\mathcal{T}} v(\boldsymbol{x}) \operatorname{rot}_{\mathcal{T}} w(\boldsymbol{x}) \mathrm{d}\boldsymbol{x} = \int_{\Omega} \boldsymbol{f}(\boldsymbol{x}) \cdot \mathcal{R}_{\mathcal{E}}^{\parallel} w(\boldsymbol{x}) \mathrm{d}\boldsymbol{x}, \ \forall w \in V_{\mathcal{E}}^{\parallel}. \tag{2.17}$$

Last, but not least we introduce a strong reconstruction operator $\hat{\mathcal{R}}_{\mathcal{T}} : \dot{X}_{\mathcal{E}} \to L^2(\Omega)^2$ which is defined for all $w \in \dot{X}_{\mathcal{E}}$ on every triangle $T \in \mathcal{T}$ by

$$\left(\hat{\mathcal{R}}_{\mathcal{T}} w\right)_{|T} = \frac{1}{|T|} \sum_{\sigma \in \mathcal{E}_T} |\sigma| w_\sigma \boldsymbol{t}_\sigma \cdot \boldsymbol{t}_{T,\sigma} \left(\boldsymbol{x}_\sigma - \boldsymbol{x}_T\right)^{\perp}.$$

This strong reconstruction operator reconstructs constant vector fields exactly, as can be seen by applying Stokes' theorem

$$\int_T \operatorname{rot} \boldsymbol{w} \mathrm{d}\boldsymbol{x} = \sum_{\sigma \in \mathcal{E}_T} \boldsymbol{t}_\sigma \cdot \boldsymbol{t}_{T,\sigma} \int_\sigma \boldsymbol{w} \cdot \boldsymbol{t}_\sigma \mathrm{d}\boldsymbol{x}$$

to $\boldsymbol{w} = \begin{pmatrix} c_1 x \\ c_2 y \end{pmatrix}^{\perp}$. Due to this fact, the reconstructed discrete velocities $\hat{\mathcal{R}}_{\mathcal{T}} v$ converge strongly in $L^2(\Omega)^2$ to the continuous solution $\boldsymbol{v}$ of the incompressible (Navier-)Stokes problem above, see the Rellich-like compactness statement in Lemma 3.5 for this.

u

2.2. Normal velocity scheme. Let us now define the normal velocity scheme. The discrete pressure space is denoted by

$$X_{\mathcal{T}} = \mathbb{R}^{\mathcal{T}}.$$

It represents the pressures at the circumcenters of the elements. For the velocity space we use the same notations $X_{\mathcal{E}}$ and $\dot{X}_{\mathcal{E}}$ as in the tangential velocity scheme, since the discrete spaces in both schemes are indeed equal. But the interpretation of the discrete velocity space is now a different one. In the tangential velocity scheme the degrees of freedom for the velocities represent the tangential velocity components at the midpoint of all the edges $\sigma \in \mathcal{E}$. Instead, in the normal velocity scheme the discrete velocities represent the corresponding normal components, now located at the midpoints of all the Voronoi faces $\sigma^{\perp}$.

Then, the normal velocity scheme reads as follows. We define

$$\operatorname{rot}_{\boldsymbol{y}} v = \frac{1}{|V_{\boldsymbol{y}}|} \sum_{\sigma \in \mathcal{E}_{\boldsymbol{y}}} |\sigma^{\perp}| v_\sigma \boldsymbol{n}_\sigma \cdot \boldsymbol{n}_{\boldsymbol{y}\sigma} \qquad \forall v \in X_{\mathcal{E}}, \ \forall \boldsymbol{y} \in \mathcal{V}, \tag{2.18}$$

$$\operatorname{div}_T v = \frac{1}{|T|} \sum_{\sigma \in \mathcal{E}_T} |\sigma| v_\sigma \boldsymbol{n}_\sigma \cdot \boldsymbol{n}_{T\sigma} \qquad \forall v \in X_{\mathcal{E}}, \ \forall T \in \mathcal{T}, \tag{2.19}$$

see again Figure 2 for the notations, and write:

find $(v, p_{\mathcal{T}}) \in \dot{X}_{\mathcal{E}} \times X_{\mathcal{T}}$ such that

$$\sum_{\boldsymbol{y} \in \mathcal{V}} |V_{\boldsymbol{y}}| \operatorname{rot}_{\boldsymbol{y}} v \operatorname{rot}_{\boldsymbol{y}} w - \sum_{T \in \mathcal{T}} |T| p_T \operatorname{div}_T w = \sum_{\sigma \in \mathcal{E}} 2 w_\sigma \int_{D_\sigma} \boldsymbol{f} \cdot \boldsymbol{n}_\sigma \mathrm{d}\boldsymbol{x}, \ \forall w \in \dot{X}_{\mathcal{E}} \tag{2.20}$$

$$\sum_{T \in \mathcal{T}} |T| p_T = 0, \tag{2.21}$$

$$\operatorname{div}_T v = 0, \ \forall T \in \mathcal{T}. \tag{2.22}$$

It is again possible to write the above scheme, using functions defined on the spatial domain Ω by

$$\operatorname{rot}_{\mathcal{V}} v(\boldsymbol{x}) = \operatorname{rot}_{\boldsymbol{y}} v \qquad \forall v \in X_{\mathcal{E}}, \ \forall \boldsymbol{y} \in \mathcal{V}, \text{for a.e. } \boldsymbol{x} \in V_{\boldsymbol{y}}, \tag{2.23}$$

$$\operatorname{div}_{\mathcal{T}} v(\boldsymbol{x}) = \operatorname{div}_T v \qquad \forall v \in X_{\mathcal{E}}, \forall T \in \mathcal{T}, \text{for a.e. } \boldsymbol{x} \in T, \tag{2.24}$$

$$\mathcal{R}_{\mathcal{E}}^{\perp} w(\boldsymbol{x}) = 2 w_\sigma \boldsymbol{n}_\sigma \qquad \forall w \in X_{\mathcal{E}}, \ \forall \sigma \in \mathcal{E}, \text{for a.e. } \boldsymbol{x} \in D_\sigma, \tag{2.25}$$

$$\mathcal{R}_{\mathcal{T}} p_{\mathcal{T}}(\boldsymbol{x}) = p_T \qquad \forall p \in X_{\mathcal{T}}, \ \forall T \in \mathcal{T}, \text{for a.e. } \boldsymbol{x} \in V_{\boldsymbol{y}}. \tag{2.26}$$

We can then rewrite (2.20)-(2.21)-(2.22) in the following way:

$$\text{find } (v, p_{\mathcal{T}}) \in \dot{X}_{\mathcal{E}} \times X_{\mathcal{T}} \text{ such that}$$

$$\int_\Omega \mathrm{rot}_{\mathcal{V}}\, v(\boldsymbol{x})\, \mathrm{rot}_{\mathcal{V}}\, w(\boldsymbol{x}) \mathrm{d}\boldsymbol{x}$$

$$-\int_\Omega \mathcal{R}_{\mathcal{T}} p_{\mathcal{T}}(\boldsymbol{x})\, \mathrm{div}_{\mathcal{T}}\, w(\boldsymbol{x}) \mathrm{d}\boldsymbol{x} = \int_\Omega \boldsymbol{f}(\boldsymbol{x}) \cdot \mathcal{R}^{\perp}_{\mathcal{E}} w(\boldsymbol{x}) \mathrm{d}\boldsymbol{x},\ \forall w \in \dot{X}_{\mathcal{E}}, \tag{2.27}$$

$$\int_\Omega \mathcal{R}_{\mathcal{T}} p_{\mathcal{T}}(\boldsymbol{x}) \mathrm{d}\boldsymbol{x} = 0, \tag{2.28}$$

$$\mathrm{div}_{\mathcal{T}}\, v(\boldsymbol{x}) = 0 \text{ for a.e. } \boldsymbol{x} \in \Omega. \tag{2.29}$$

It is again possible to write Problem (2.13)-(2.14)-(2.15) without using the pressure. We denote by

$$V^{\perp}_{\mathcal{E}} = \{v \in \dot{X}_{\mathcal{E}}, \mathrm{div}_{\mathcal{T}}\, v = 0\}. \tag{2.30}$$

We then notice that a solution of Problem (2.27)-(2.28)-(2.29) also satisfies

$$v \in V^{\perp}_{\mathcal{E}}, \int_\Omega \mathrm{rot}_{\mathcal{V}}\, v(\boldsymbol{x})\, \mathrm{rot}_{\mathcal{V}}\, w(\boldsymbol{x}) \mathrm{d}\boldsymbol{x} = \int_\Omega \boldsymbol{f}(\boldsymbol{x}) \cdot \mathcal{R}^{\perp}_{\mathcal{E}} w(\boldsymbol{x}) \mathrm{d}\boldsymbol{x},\ \forall w \in V^{\perp}_{\mathcal{E}}. \tag{2.31}$$

Similar to the tangential velocity scheme, we introduce also a strong reconstruction operator $\hat{\mathcal{R}}_{\mathcal{V}} : \dot{X}_{\mathcal{E}} \to L^2(\Omega)^2$ for the normal velocity scheme which is defined for all $w \in \dot{X}_{\mathcal{E}}$ at every interior node $\boldsymbol{y} \in \mathcal{V}$ by

$$\left(\hat{\mathcal{R}}_{\mathcal{V}} w\right)|_{V_{\boldsymbol{y}}} = \frac{1}{|V_{\boldsymbol{y}}|} \sum_{\sigma \in \mathcal{E}_{\boldsymbol{y}}} |\sigma^{\perp}| w_\sigma \boldsymbol{n}_\sigma \cdot \boldsymbol{n}_{\boldsymbol{y}\sigma} \left(\boldsymbol{x}_{\sigma^\perp} - \boldsymbol{x}_T\right)^{\perp}.$$

Similar to the tangential velocity scheme, also this strong reconstruction operator reconstructs constant vector fields exactly.

3. Mathematical analysis of the tangential velocity scheme

In order to write a discrete equivalent of the continuous Helmholtz decomposition, which will be applied to scheme (2.6)-(2.7)-(2.8), we introduce the following additional notations.

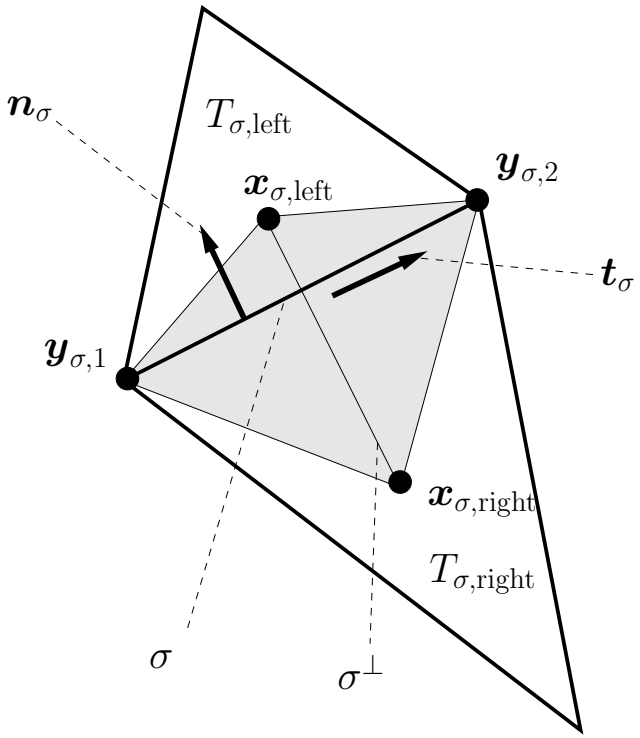

FIGURE 3. Tangential velocity scheme: notations for the discrete Helmholtz decomposition

For a given edge $\sigma \in \mathcal{E}$ connecting the two vertices $\boldsymbol{y}_{\sigma,1}$ and $\boldsymbol{y}_{\sigma,2}$, the unit vector $\boldsymbol{t}_\sigma$ is directed along the edge and points from the former vertex to the latter, see Figure 3. We denote, for an interior

edge σ by $\boldsymbol{x}_{\sigma,\text{left}}$ and $\boldsymbol{x}_{\sigma,\text{right}}$ the circumcenters of the triangles $T_{\sigma,\text{left}}$ and $T_{\sigma,\text{right}}$ adjacent to the edge σ, and we set $u_{T_{\sigma,\text{right}}} = 0$ for a boundary edge σ. Here, the definition of left and right is chosen according to the orientation $\boldsymbol{t}_\sigma$ of the edge.

For a given triangle $T \in \mathcal{T}$ and $\sigma \in \mathcal{E}_T$, $\boldsymbol{x}_{T,\sigma}$, denotes the circumcenter of the triangle adjacent to T through σ, and $u_{T,\sigma}$ denotes the corresponding value of a function u.

Similarly, for a Voronoi box V_y around $y \in \mathcal{V}$ and an edge $\sigma \in \mathcal{E}_y$, y_σ denotes the vertex at the end of σ opposite to y, and $q_{y,\sigma}$ the corresponding value of a function q.

We then define

$$\text{curl}^{\parallel}_\sigma u = \frac{u_{T_{\sigma,\text{left}}} - u_{T_{\sigma,\text{right}}}}{|\sigma^\perp|} \qquad \forall u \in X_{\mathcal{T}},\ \forall \sigma \in \mathcal{E}, \tag{3.1}$$

$$\Delta_T u = \frac{1}{|T|} \sum_{\sigma \in \mathcal{E}_T} |\sigma| \frac{u_{T,\sigma} - u_T}{|\sigma^\perp|} \qquad \forall u \in X_{\mathcal{T}},\ \forall T \in \mathcal{T}, \tag{3.2}$$

$$\text{grad}^{\parallel}_\sigma q = \frac{q_{\boldsymbol{y}_{\sigma,2}} - q_{\boldsymbol{y}_{\sigma,1}}}{|\sigma|} \qquad \forall q \in X_{\mathcal{V}},\ \forall \sigma \in \mathcal{E}, \tag{3.3}$$

$$\Delta_{\boldsymbol{y}} q = \frac{1}{V_{\boldsymbol{y}}} \sum_{\sigma \in \mathcal{E}_{\boldsymbol{y}}} |\sigma^\perp| \frac{q_{\boldsymbol{y},\sigma} - q_{\boldsymbol{y}}}{|\sigma|} \qquad \forall q \in X_{\mathcal{V}},\ \forall \boldsymbol{y} \in \mathcal{V}. \tag{3.4}$$

Remark 3.1. The discrete operators $\text{grad}^{\parallel}_\sigma q$ and $\text{curl}^{\parallel}_\sigma u$ deliver approximations of the directional gradient $\nabla q \cdot \boldsymbol{t}_\sigma$ along the edge σ, and the corresponding directional curl operator $\text{curl}\, u \cdot \boldsymbol{t}_\sigma = \nabla u \cdot \boldsymbol{n}_\sigma$.

We then have the following lemma.

Lemma 3.2 (Helmholtz decomposition, tangential velocity scheme). *Under hypothesis* (1.5)*, let* $\mathcal{M} = (\mathcal{V}, \mathcal{E}, \mathcal{T})$ *be a mesh of the domain* Ω *in the sense of Definition 2.1. Then for all* $v \in X_{\mathcal{E}}$*, there exists one and only one* $(u, q) \in X_{\mathcal{T}} \times X_{\mathcal{V}}$ *such that*

$$v_\sigma = \text{curl}^{\parallel}_\sigma u + \text{grad}^{\parallel}_\sigma q,\ \forall \sigma \in \mathcal{E}, \tag{3.5}$$

$$\sum_{\boldsymbol{y} \in \mathcal{V}} |V_{\boldsymbol{y}}| q_{\boldsymbol{y}} = 0. \tag{3.6}$$

We then denote $u = U^{\parallel}(v)$ *and* $q = Q^{\parallel}(v)$*. Moreover, if* $v \in V^{\parallel}_{\mathcal{E}}$*, we have* $q = 0$ *and* $u \in X_{\mathcal{T},0}$*, where we define*

$$X_{\mathcal{T},0} = \{u \in X_{\mathcal{T}}, u_T = 0,\ \textit{for all } T \in \mathcal{T} \textit{ with } \mathcal{E}_T \cap \mathcal{E}_{\text{bnd}} \neq \emptyset\}. \tag{3.7}$$

Proof. Let us first remark that, thanks to Euler's relation, we have

$$\#\mathcal{V} + \#\mathcal{T} = \#\mathcal{E} + 1.$$

Since the linear system (3.5)-(3.6) contains $\#\mathcal{E} + 1$ equations, it suffices to prove the uniqueness of (u, q) for proving at the same time the existence. We then remark that, plugging (3.5) into (2.4), the terms in q vanish, and we get

$$-\Delta_T u = \text{rot}_T\, v,\ \forall T \in \mathcal{T}.$$

Setting $v = 0$, multiplying by u_T and summing on $T \in \mathcal{T}$ leads to

$$\sum_{\sigma \in \mathcal{E}_{\text{int}}} \frac{|\sigma|}{|\sigma^\perp|} (u_{T_{\sigma,\text{left}}} - u_{T_{\sigma,\text{right}}})^2 + \sum_{\sigma \in \mathcal{E}_{\text{bnd}}} \frac{|\sigma|}{|\sigma^\perp|} (u_{T_{\sigma,\text{left}}})^2 = 0,$$

which shows that $u = 0$ (hence we recover the standard result of the uniqueness of the solution of the discrete finite volume Laplace operator with homogeneous Dirichlet boundary condition on $\mathcal{T}$, as given in [**4**]). This proves that $u \in X_{\mathcal{T}}$ is uniquely defined. We then introduce (3.5) into (2.5), and we observe that the terms in u vanish, leading to

$$\Delta_{\boldsymbol{y}} q = \text{div}_{\boldsymbol{y}}\, v,\ \forall \boldsymbol{y} \in \mathcal{V}.$$

Setting $v = 0$, multiplying by $q_{\boldsymbol{y}}$ and summing on $\boldsymbol{y} \in \mathcal{V}$ leads to

$$\sum_{\sigma \in \mathcal{E}} \frac{|\sigma^\perp|}{|\sigma|} (q_{\boldsymbol{y}_{\sigma,2}} - q_{\boldsymbol{y}_{\sigma,1}})^2 = 0,$$

showing that q takes a constant value for all $\boldsymbol{y} \in \mathcal{V}$. Thanks to the condition (3.6), we get that this constant value is zero (hence we recover the standard result of the uniqueness of the solution

whose mean value is equal to zero, to the discrete finite volume Laplace operator with homogeneous Neumann boundary condition on the finite volume mesh $\{V_{\boldsymbol{y}}, \boldsymbol{y} \in \mathcal{V}\}$, see [**4**]). This proves that $q \in X_{\mathcal{V}}$ is uniquely defined. Taking $v \in V_{\mathcal{E}}^{\parallel}$, we have $\mathrm{div}_{\mathcal{V}} v = 0$, and therefore $Q^{\parallel}(v) = 0$. Since $V_{\mathcal{E}}^{\parallel} \subset \dot{X}_{\mathcal{E}}$, we have $v_\sigma = 0$ for all $\sigma \in \mathcal{E}_{\mathrm{bnd}}$. Therefore, since

$$v_\sigma = \frac{u_{T_{\sigma,\mathrm{left}}} - u_{T_{\sigma,\mathrm{right}}}}{|\sigma^\perp|},$$

and $u_{T_{\sigma,\mathrm{right}}} = 0$ for all $\sigma \in \mathcal{E}_{\mathrm{bnd}}$, we get $u_{T_{\sigma,\mathrm{left}}} = 0$, which proves that $u \in X_{\mathcal{T},0}$. □

We now have the following property.

Lemma 3.3 (Streamline potential formulation, tangential velocity scheme). *Under hypothesis* (1.5)*, let $\mathcal{M} = (\mathcal{V}, \mathcal{E}, \mathcal{T})$ be a mesh of the domain Ω in the sense of Definition 2.1. Then $v \in V_{\mathcal{E}}^{\parallel}$ is a solution of* (2.17) *if and only if $u = U^{\parallel}(v)$, as defined by Lemma 3.2 is a solution to*

$$u \in X_{\mathcal{T},0}, \forall w \in X_{\mathcal{T},0}, \int_\Omega \Delta_{\mathcal{T}} u(\boldsymbol{x}) \Delta_{\mathcal{T}} w(\boldsymbol{x}) \mathrm{d}\boldsymbol{x} = \int_\Omega \rho_{\frac{\pi}{2}} \boldsymbol{f}(\boldsymbol{x}) \cdot \nabla_{\mathcal{E}} w(\boldsymbol{x}) \mathrm{d}\boldsymbol{x}, \tag{3.8}$$

where

$$\Delta_{\mathcal{T}} u(\boldsymbol{x}) = \Delta_T u, \ \textit{for a.e. } \boldsymbol{x} \in V_T, \forall T \in \mathcal{T}, \tag{3.9}$$

$$\nabla_{\mathcal{E}} w(\boldsymbol{x}) = 2 \frac{w_{T_{\sigma,left}} - w_{T_{\sigma,right}}}{|\sigma^\perp|} \boldsymbol{n}_\sigma, \ \textit{for a.e. } \boldsymbol{x} \in D_\sigma, \forall \sigma \in \mathcal{E}, \ \forall w \in X_{\mathcal{E}}. \tag{3.10}$$

As a consequence, there exists one and only one solution $v \in V_{\mathcal{E}}^{\parallel}$ to (2.17)*, defined by $v = \mathrm{curl}_{\mathcal{E}}^{\parallel} u$.*

Proof. It suffices to take $\mathrm{curl}_{\mathcal{E}}^{\parallel} w$ as test function in (2.17).

Since $\mathrm{div}_{\mathcal{V}} \mathrm{curl}_{\mathcal{E}}^{\parallel} w = 0$, and since $\boldsymbol{n}_\sigma = \rho_{\frac{\pi}{2}} \boldsymbol{t}_\sigma$, we get (3.8). Reciprocally, assuming that u is solution to (3.8), we get, since $Q^{\parallel}(w) = 0$ for all elements of $V_{\mathcal{E}}^{\parallel}$, that $v = \mathrm{curl}_{\mathcal{E}}^{\parallel} u$ is solution to (2.17). We then apply the discrete existence and uniqueness result for a discrete biharmonic problem given in [**6**], which provides that Problem (3.8) with Definition (3.10) has one and only one solution. □

Let us now state two direct consequences of the results proven in [**6**].

Lemma 3.4. *Under hypothesis* (1.5)*, let $\boldsymbol{w} \in C_c^\infty(\Omega)^2$ be given with $\nabla \cdot \boldsymbol{w} = 0$ (where we denote by $C_c^\infty(\Omega)$ the set of infinitely differentiable functions with compact support in Ω) and let $\mathcal{M} = (\mathcal{V}, \mathcal{E}, \mathcal{T})$ be a given discretization in the sense of Definition 2.1. Then there exists a quasi-interpolation operator $\hat{\mathcal{I}}_{\mathcal{M}}^{\parallel} : C_c^\infty(\Omega)^2 \to V_{\mathcal{E}}^{\parallel}$ such that*

$$\|\hat{\mathcal{R}}_{\mathcal{T}} \hat{\mathcal{I}}_{\mathcal{M}}^{\parallel} \boldsymbol{w} - \boldsymbol{w}\|_{L^2(\Omega)^2} \leq C_{\boldsymbol{w}} h_{\mathcal{M}} \tag{3.11}$$

$$\|\mathrm{rot}_{\mathcal{T}} \hat{\mathcal{I}}_{\mathcal{M}}^{\parallel} \boldsymbol{w} - \mathrm{rot}\, \boldsymbol{w}\|_{L^2(\Omega)} \leq C_{\boldsymbol{w}} h_{\mathcal{M}}, \tag{3.12}$$

where $C_{\boldsymbol{w}}$ only depends on $\boldsymbol{w}$ and on any $\theta > 0$ such that $\theta \leq \theta_{\mathcal{M}}$. Moreover, $\mathcal{R}_{\mathcal{E}}^{\parallel} \hat{\mathcal{I}}_{\mathcal{M}}^{\parallel} \boldsymbol{w}$ converges weakly to $\boldsymbol{w}$ in $L^2(\Omega)^2$ as $h_{\mathcal{M}} \to 0$ under the condition $\theta \leq \theta_{\mathcal{M}}$.

Proof. We consider the discrete stream function v defined by Lemma 3.3 of [**6**] for $f = \mathrm{rot}\, w$ and define $(\mathcal{I}_{\mathcal{M}}^{\parallel} w)|_\sigma := \mathrm{curl}_\sigma v$. Equation (31) of [**6**] gives (3.12). Estimate (3.11) is obtained using the result on the strong discrete reconstruction of the gradient of the discrete stream function, provided in [**5**]. □

We prove weak compactness for discretely divergence-free velocities, with bounded discrete rotation.

Lemma 3.5. *Under hypothesis* (1.5)*, let us denote*

$$\|v_n\|_{X_{\mathcal{E}_n}^{\parallel}} := \sqrt{\|\mathrm{rot}_{\mathcal{T}_n} v_n\|_{L^2(\Omega)}^2 + \|\mathrm{div}_{\mathcal{V}_n} v_n\|_{L^2(\Omega)}^2}. \tag{3.13}$$

We assume that $(\mathcal{M}_n)_{n \in \mathbb{N}}$ is a sequence such that:

- *$\mathcal{M}_n = (\mathcal{V}_n, \mathcal{E}_n, \mathcal{T}_n)$ is a discretization in the sense of Definition 2.1,*
- *$h_{\mathcal{M}_n}$ tends to 0 as n tends to ∞ and $\theta_{\mathcal{M}_n} \geq \theta > 0$,*

- *for all $n \in \mathbb{N}$, there exists $v_n \in V_{\mathcal{E}_n}^{\|}$, such that there exists $C > 0$, independent of n, with $\|v_n\|_{X_{\mathcal{E}_n}} = \|\mathrm{rot}_{\mathcal{T}_n} v_n\|_{L^2(\Omega)} \leq C$.*

Then there exists $\boldsymbol{v} \in H_0^1(\Omega)^2$ with $\nabla \cdot \boldsymbol{v} = 0$ and a subsequence of $(\mathcal{M}_n)_{n\in\mathbb{N}}$, again denoted by $(\mathcal{M}_n)_{n\in\mathbb{N}}$, such that

- $\mathrm{rot}_{\mathcal{T}_n} v_n \rightharpoonup \mathrm{rot}\, \boldsymbol{v}$ *weakly in* $L^2(\Omega)$,
- $\mathcal{R}_{\mathcal{E}_n}^{\|} v_n \rightharpoonup \boldsymbol{v}$ *weakly in* $L^2(\Omega)^2$,
- $\hat{\mathcal{R}}_{\mathcal{T}_n} v_n \longrightarrow \boldsymbol{v}$ *strongly in* $L^2(\Omega)^2$.

Proof. The proof of this lemma is obtained by using the discrete stream function given by Lemma 3.2, and then to apply Lemma 3.2 of [**6**], where the corresponding compactness properties for a discrete biharmonic problem are proven. Note that the weak convergence of the Laplacian there corresponds to the weak convergence of the rotation here, due to $\boldsymbol{v} = \mathrm{curl}\, \xi$ and $\mathrm{rot}\, \mathrm{curl}\, \xi = -\Delta \xi$. □

Now, we can state the convergence theorem.

Theorem 3.6. *Let $\mathcal{M} = (\mathcal{V}, \mathcal{E}, \mathcal{T})$ be a discretization in the sense of Definition 2.1, and let $\boldsymbol{f} \in L^2(\Omega)^2$. Then there exists one and only one $v \in V_{\mathcal{E}}^{\|}$ such that (2.17) holds. Moreover, assuming that $h_{\mathcal{M}}$ tends to 0 while $\theta_{\mathcal{M}} \geq \theta$ for some $\theta > 0$, then $\boldsymbol{v} \in H_0^1(\Omega)^2$ denoting the weak solution of Problem (1.1)-(1.4) converges in the following sense*

- $\mathrm{rot}_{\mathcal{T}} v \longrightarrow \mathrm{rot}\, \boldsymbol{v}$ *in* $L^2(\Omega)$,
- $\mathcal{R}_{\mathcal{E}}^{\|} v \rightharpoonup \boldsymbol{v}$ *weakly in* $L^2(\Omega)^2$,
- $\hat{\mathcal{R}}_{\mathcal{T}} v \longrightarrow \boldsymbol{v}$ *strongly in* $L^2(\Omega)^2$.

Proof. Let us first write an a-priori estimate on the approximate solution. We let $w = v$ in (2.17). We get

$$\int_\Omega (\mathrm{rot}_{\mathcal{T}}\, v)^2 \mathrm{d}\boldsymbol{x} = \int_\Omega \boldsymbol{f} \cdot \mathcal{R}_{\mathcal{E}}^{\|} v \mathrm{d}\boldsymbol{x}. \tag{3.14}$$

We now apply the Cauchy-Schwarz inequality to the right hand side of the above equation. Recalling the definition (3.13), we get

$$\|v\|_{X_{\mathcal{E}}^{\|}}^2 \leq \|\boldsymbol{f}\|_{L^2(\Omega)^2} \|\mathcal{R}_{\mathcal{E}}^{\|} v\|_{L^2(\Omega)^2} \leq C_1 \|\boldsymbol{f}\|_{L^2(\Omega)^2} \|v\|_{X_{\mathcal{E}}^{\|}}.$$

This provides

$$\|v\|_{X_{\mathcal{E}}^{\|}} \leq C_1 \|\boldsymbol{f}\|_{L^2(\Omega)^2}$$

and shows that scheme (2.17) has one and only one solution, since it is equivalent to a square linear system whose unknowns are the degrees of freedom in the vector space $V_{\mathcal{E}}^{\|}$. Indeed, it suffices to take $\boldsymbol{f} = 0$. Then, the previous inequality shows that $v = 0$ holds. We now remark that the previous inequality allows to apply Lemma 3.5. Therefore, taking a sequence of discretizations $(\mathcal{M}_n)_{n\in\mathbb{N}}$ such that $h_{\mathcal{M}_n}$ tends to 0 as n tends to ∞ and $\theta_{\mathcal{M}_n} \geq \theta > 0$, we get the existence of a subsequence (denoted by the same notation) and of $\boldsymbol{v} \in H_0^1(\Omega)^2$ such that the conclusions of Lemma 3.5 hold.

Let $\boldsymbol{w} \in C_c^\infty(\Omega)^2$ be given with $\nabla \cdot \boldsymbol{w} = 0$, and let us apply the quasi-interpolation operator $\hat{\mathcal{I}}_{\mathcal{M}_n}^{\|} \boldsymbol{w} \in V_{\mathcal{E}}^{\|}$ from Lemma 3.4 to (2.17). We get

$$\int_\Omega \mathrm{rot}_{\mathcal{T}_n} v_n\, \mathrm{rot}_{\mathcal{T}_n} \hat{\mathcal{I}}_{\mathcal{M}_n} \boldsymbol{w} \mathrm{d}\boldsymbol{x} = \int_\Omega \boldsymbol{f} \cdot \mathcal{R}_{\mathcal{E}_n}^{\|} \hat{\mathcal{I}}_{\mathcal{M}_n} \boldsymbol{w} \mathrm{d}\boldsymbol{x}.$$

Thanks to Lemmas 3.4 and 3.5, we may pass to the limit $n \to \infty$ in the above equation, since the use of both lemmas provides standard weak/strong convergence in the left hand side, and the weak convergence result of Lemma 3.4. We then get

$$\int_\Omega \mathrm{rot}\, \boldsymbol{v}\, \mathrm{rot}\, \boldsymbol{w} \mathrm{d}\boldsymbol{x} = \int_\Omega \boldsymbol{f} \cdot \boldsymbol{w} \mathrm{d}\boldsymbol{x}.$$

According to a density theorem given by Temam [**26**], the smooth divergence-free functions functions are dense in the set of all divergence-free $H_0^1(\Omega)^2$ functions, which proves that $\boldsymbol{v}$ is the unique weak solution of Problem (1.1)-(1.4). A standard reasoning then shows that the entire sequence converges, which leads to the convergence of the scheme. It now remains to prove the convergence of $\mathrm{rot}_{\mathcal{T}}\, v$ to

$\mathrm{rot}\,\boldsymbol{v}$ in $L^2(\Omega)$. Passing to the limit in (2.17), with $v = w = v_n$, we get that the limit of $\|v_n\|^2_{X^{\|}_{\mathcal{E}_n}}$ is equal to $\int_\Omega \boldsymbol{f}\cdot\boldsymbol{v}\mathrm{d}\boldsymbol{x} = \|\mathrm{rot}\,\boldsymbol{v}\|^2_{L^2(\Omega)}$. This, in addition to the weak convergence result given by Lemma 3.5, proves the strong convergence of $\mathrm{rot}_{\mathcal{T}}\, v$. □

4. Mathematical analysis of the normal velocity scheme

Let us write the following discrete equivalent of Helmholtz decomposition, which will be applied to scheme (2.20)-(2.21)-(2.22). Using the same notations as above, we define

$$\mathrm{curl}^{\perp}_{\sigma} u = -\,\mathrm{grad}^{\|}_{\sigma} u \qquad \forall u \in X_{\mathcal{V}},\ \forall \sigma \in \mathcal{E}, \tag{4.1}$$

$$\mathrm{grad}^{\perp}_{\sigma} q = \mathrm{curl}^{\|}_{\sigma} q \qquad \forall q \in X_{\mathcal{T}},\ \forall \sigma \in \mathcal{E}. \tag{4.2}$$

Remark 4.1. Similar to the tangential velocity scheme, the discrete operators $\mathrm{grad}^{\perp}_{\sigma} q$ and $\mathrm{curl}^{\perp}_{\sigma} u$ deliver approximations of the directional gradient $\nabla q\cdot\boldsymbol{n}_\sigma$, and the corresponding directional curl operator $\mathrm{curl}\, u\cdot\boldsymbol{n}_\sigma = -\nabla u\cdot\boldsymbol{t}_\sigma$.

We then have the following lemma:

Lemma 4.2 (Discrete Helmholtz decomposition, normal velocity scheme). *Under hypothesis* (1.5)*, let $\mathcal{M} = (\mathcal{V},\mathcal{E},\mathcal{T})$ be a mesh of the domain Ω in the sense of Definition 2.1. Then for all $v \in X_{\mathcal{E}}$, there exists one and only one $(u,q) \in X_{\mathcal{V}}\times X_{\mathcal{T}}$ such that*

$$v_\sigma = \mathrm{curl}^{\perp}_{\sigma} u + \mathrm{grad}^{\perp}_{\sigma} q,\ \forall \sigma\in\mathcal{E}, \tag{4.3}$$

$$\sum_{\sigma\in\mathcal{E}_{\mathrm{bnd}}}\sum_{\boldsymbol{y}\in\mathcal{V}_\sigma} |\sigma| u_{\boldsymbol{y}} = 0. \tag{4.4}$$

We then denote $u = U^{\perp}(v)$ and $q = Q^{\perp}(v)$. Moreover, if $v \in V^{\perp}_{\mathcal{E}}$, $q = 0$ and $u \in X_{\mathcal{V},0}$, where we define

$$X_{\mathcal{V},0} = \{u \in X_{\mathcal{V}}, u_{\boldsymbol{y}} = 0,\ \textit{for all } \boldsymbol{y}\in\mathcal{V}_{\mathrm{bnd}} \neq \emptyset\}. \tag{4.5}$$

Proof. Following the same ideas as in Lemma 3.2, exchanging the roles of u and q, two Laplace problems must be considered. The Laplace problem in q happens to be a standard finite volume discretization of a homogeneous Dirichlet problem (the unknowns are cell-centered). On the contrary, the Laplace problem for u is a homogeneous Neumann problem, where the constant is fixed by condition (4.4) instead of condition (3.6). In the case $v \in V^{\perp}_{\mathcal{E}}$, we get that $u_{\boldsymbol{y}}$ is constant on $\partial\Omega$. Thanks to the condition (4.4), we get that, for $v \in V^{\perp}_{\mathcal{E}}$, then the average value of $u_{\boldsymbol{y}}$ on $\partial\Omega$ is equal to zero. and therefore this constant is equal to zero.

Note that $\Delta_{\boldsymbol{y}} u$ is identical to the P_1-Laplacian, since $|\sigma^{\perp}|/|\sigma| = -\int_\Omega \xi_{\boldsymbol{y}_{\sigma,1}}\cdot\xi_{\boldsymbol{y}_{\sigma,2}}\mathrm{d}\boldsymbol{x}$, the term of the stiffness matrix issued from the use of the piecewise affine basis functions $\xi_{\boldsymbol{y}}$, equal to 1 at vertex $\boldsymbol{y}$ and to 0 at all other vertices, see also [**4, 12**]. This will allow us for applying the results given in [**7**]. □

We now have the following property.

Lemma 4.3 (Formulation in streamline potential, normal velocity scheme). *Under hypothesis* (1.5)*, let $\mathcal{M} = (\mathcal{V},\mathcal{E},\mathcal{T})$ be a mesh of the domain Ω in the sense of Definition 2.1. Then $v \in V^{\perp}_{\mathcal{E}}$ is a solution of* (2.31) *if and only if $u = U^{\perp}(v)$, as defined by Lemma 4.2 is solution to*

$$u \in X_{\mathcal{V},0}, \forall w \in X_{\mathcal{V},0}, \int_\Omega \Delta_{\mathcal{V}} u(\boldsymbol{x})\Delta_{\mathcal{V}} w(\boldsymbol{x})\mathrm{d}\boldsymbol{x} = \int_\Omega \rho_{\frac{\pi}{2}}\boldsymbol{f}(\boldsymbol{x})\cdot\nabla_{\mathcal{E}} w(\boldsymbol{x})\mathrm{d}\boldsymbol{x}, \tag{4.6}$$

where

$$X_{\mathcal{V},0} := \{u \in X_{\mathcal{V}}, u_{\boldsymbol{y}} = 0\, \textit{for all}\, \boldsymbol{y}\in\mathcal{V}_{\mathrm{bnd}}\}, \tag{4.7}$$

$$\Delta_{\mathcal{V}} u(\boldsymbol{x}) = \Delta_{\boldsymbol{y}} u,\ \textit{for a.e. } \boldsymbol{x}\in V_{\boldsymbol{y}}, \forall \boldsymbol{y}\in\mathcal{V}, \tag{4.8}$$

$$\nabla_{\mathcal{E}} w(\boldsymbol{x}) = 2\frac{w_{\boldsymbol{y}_{\sigma,2}} - w_{\boldsymbol{y}_{\sigma,1}}}{|\sigma|}\boldsymbol{t}_\sigma,\ \textit{for a.e. } \boldsymbol{x}\in D_\sigma, \forall\sigma\in\mathcal{E},\ \forall w\in X_{\mathcal{E}}. \tag{4.9}$$

As a consequence, there exists one and only one solution $v \in V^{\perp}_{\mathcal{E}}$ to (2.31)*, defined by $v = \mathrm{curl}^{\perp}_{\mathcal{E}} u$.*

PROOF. It suffices to take $\operatorname{curl}_{\mathcal{E}}^{\perp} w$ as test function in (2.31).

Since $\operatorname{div}_{\mathcal{V}} \operatorname{curl}_{\mathcal{E}}^{\perp} w = 0$, and since $\boldsymbol{n}_\sigma = \rho_{\frac{\pi}{2}} \boldsymbol{t}_\sigma$, we get (4.6). Reciprocally, assuming that u is solution to (4.6), we get, since $Q(w) = 0$ for all elements of $V_{\mathcal{E}}$, that $v = \operatorname{curl}_{\mathcal{E}}^{\perp} u$ is solution to (2.31). We then apply the result given in [**7**], which provides that Problem (4.6) with Definition (4.9) has one and only one solution. □

For the normal velocity scheme we can prove a discrete inf-sup stability, which we will formulate as a discrete variant of divergence-stability. For that, we introduce the following discrete H^1-norm for $v \in \dot{X}_{\mathcal{E}}$

$$\|v\|_{X_{\mathcal{E}}^{\perp}} := \sqrt{\|\operatorname{rot}_{\mathcal{V}} v\|_{L^2(\Omega)}^2 + \|\operatorname{div}_{\mathcal{T}} v\|_{L^2(\Omega)}^2}, \tag{4.10}$$

and we apply the following technical lemma:

LEMMA 4.4. *For a given triangle T, and a weakly differentiable function $g \in H^1(T)$, we define for every edge σ of the triangle, its face average*

$$\bar{g}_\sigma := \frac{1}{|\sigma|} \int_\sigma g(\boldsymbol{x}) \mathrm{d}\gamma(\boldsymbol{x}).$$

Then, we can estimate the difference of the face averages of two of its faces by

$$(\bar{g}_{\sigma_1} - \bar{g}_{\sigma_2})^2 \leq C_{\mathrm{geom}} \frac{\operatorname{diam}(T)}{|\sigma_1| + |\sigma_2|} \int_T |\nabla g(\boldsymbol{x})|^2.$$

PROOF. We introduce the volume average

$$\bar{g}_T := \frac{1}{|T|} \int_T g(\boldsymbol{x}) \mathrm{d}(\boldsymbol{x}),$$

and estimate

$$(\bar{g}_{\sigma_1} - \bar{g}_{\sigma_2})^2 \leq 2\,(\bar{g}_{\sigma_1} - \bar{g}_T)^2 + 2\,(\bar{g}_{\sigma_2} - \bar{g}_T)^2\,.$$

Then, the estimate follows directly from the proof of lemma 9.4 in [**4**]. □

LEMMA 4.5 (Discrete inf-sup stability of the normal velocity scheme). *For a given discrete pressure $q \in X_{\mathcal{T}}$ with $\int_\Omega \mathcal{R}_{\mathcal{T}} q(\boldsymbol{x}) \mathrm{d}\boldsymbol{x} = 0$, we find a discrete velocity $w_q \in \dot{X}_{\mathcal{E}}$ such that*

$$\operatorname{div}_{\mathcal{T}} w_q = q, \tag{4.11}$$

$$\|w_q\|_{X_{\mathcal{E}}^{\perp}} \leq C_N \|q\|_{L^2(\Omega)} \tag{4.12}$$

hold. Here, C_N is independent of the mesh size and can be interpreted as the inverse of a discrete inf-sup constant.

PROOF. The discrete pressure q is piecewise constant, has zero average and is square-integrable. Therefore, we find a continuous Nečas lifting $\boldsymbol{w}_q \in H_0^1(\Omega)^2$ such that

$$\nabla \cdot \boldsymbol{w}_q = q$$

and

$$\|\nabla \boldsymbol{w}_q\|_{L^2(\Omega)^{2\otimes 2}} \leq \frac{1}{\beta} \|q\|_{L^2(\Omega)}$$

hold, where β is the continuous inf-sup constant of the domain Ω. Now the average of $\boldsymbol{w}_q$ on every edge is defined, since $\boldsymbol{w}_q \in H_0^1(\Omega)^2$ has a well-defined trace in $L^2(\sigma)^2$ and we denote it by

$$\bar{\boldsymbol{w}}_{q_\sigma} := \frac{1}{|\sigma|} \int_\sigma \boldsymbol{w}_q \mathrm{d}\gamma(\boldsymbol{x}).$$

The discrete Nečas lifting $w_q \in \dot{X}_{\mathcal{E}}$ on every edge $\sigma \in \mathcal{E}$ is then simply defined by

$$w_{q_\sigma} = \bar{\boldsymbol{w}}_{q_\sigma} \cdot \boldsymbol{n}_\sigma.$$

We remark that for all boundary edges $\sigma \in \mathcal{E}_{\mathrm{bnd}}$ indeed $w_{q_\sigma} = 0$ and $w_q \in \dot{X}_{\mathcal{E}}$ hold. We then have the property

$$\operatorname{div}_T w_q = \frac{1}{|T|} \int_T \mathcal{R}_{\mathcal{T}} q(\boldsymbol{x}) \mathrm{d}\boldsymbol{x} = q_T$$

due to the Gauss theorem for the continuous divergence, and we see that (4.11) holds for w_q. We now have to show (4.12) for w_q. Using

$$\|w_q\|^2_{X^\perp_{\mathcal{E}}} = \|\mathrm{div}_{\mathcal{T}}\, w_q\|^2_{L^2(\Omega)} + \|\mathrm{rot}_{\mathcal{V}}\, w_q\|^2_{L^2(\Omega)} = \|q\|^2_{L^2(\Omega)} + \|\mathrm{rot}_{\mathcal{V}}\, w_q\|^2_{L^2(\Omega)},$$

we see that we have to estimate the discrete rotation of w_q.

First, we regard the discrete rotation around an interior point $\boldsymbol{y} \in \mathcal{V}_{\boldsymbol{y}}$. Therefore, we define a (vector-valued) average of all the $\bar{\boldsymbol{w}}_{q_\sigma}$ around $\boldsymbol{y}$ by

$$\bar{\boldsymbol{w}}_{q_{\boldsymbol{y}}} := \frac{\sum_{\sigma' \in \mathcal{E}_{\boldsymbol{y}}} |\sigma'| \bar{\boldsymbol{w}}_{q_{\sigma'}}}{\sum_{\sigma' \in \mathcal{E}_{\boldsymbol{y}}} |\sigma'|}.$$

Now we write the rotation around an interior point $\boldsymbol{y}$ as

$$\begin{aligned}\mathrm{rot}_{\boldsymbol{y}}\, w_q &= \frac{1}{|V_{\boldsymbol{y}}|} \sum_{\sigma \in \mathcal{E}_\sigma} |\sigma^\perp| w_{q_\sigma} \boldsymbol{n}_\sigma \cdot \boldsymbol{n}_{\boldsymbol{y}\sigma} \\ &= \frac{1}{|V_{\boldsymbol{y}}|} \sum_{\sigma \in \mathcal{E}_\sigma} |\sigma^\perp| \bar{\boldsymbol{w}}_{q_\sigma} \cdot \boldsymbol{n}_{\boldsymbol{y}\sigma} - \frac{1}{|V_{\boldsymbol{y}}|} \sum_{\sigma \in \mathcal{E}_\sigma} |\sigma^\perp| \bar{\boldsymbol{w}}_{q_{\boldsymbol{y}}} \cdot \boldsymbol{n}_{\boldsymbol{y}\sigma},\end{aligned}$$

since the rotation of the constant vector $\bar{\boldsymbol{w}}_{q_{\boldsymbol{y}}}$ is zero. This expression can further be transformed into

$$\mathrm{rot}_{\boldsymbol{y}}\, w_q = \frac{1}{|V_{\boldsymbol{y}}|} \sum_{\sigma \in \mathcal{E}_\sigma} \frac{|\sigma^\perp|}{\sum_{\sigma' \in \mathcal{E}_{\boldsymbol{y}}} |\sigma'|} \left(\sum_{\sigma' \in \mathcal{E}_{\boldsymbol{y}}} |\sigma'| (\bar{\boldsymbol{w}}_{q_\sigma} - \bar{\boldsymbol{w}}_{q'_\sigma}) \cdot \boldsymbol{n}_{\boldsymbol{y}\sigma} \right).$$

We now assume that the edges of the set $\mathcal{E}_{\boldsymbol{y}}$ are indexed by $1, 2, \ldots, |\mathcal{E}_{\boldsymbol{y}}|$ and that they are oriented in a counterclockwise manner around $\boldsymbol{y}$. Further, we assume that there are mappings $\sigma_{\boldsymbol{y}}(i)$ and $\sigma_{\boldsymbol{y}}(i+1)$ which map the indices onto $\mathcal{E}_{\boldsymbol{y}}$. Here, $\sigma_{\boldsymbol{y}}(i+1)$ maps the index i onto the edge which is the neighbor edge of $\sigma_{\boldsymbol{y}}(i)$ in counterclockwise orientation. Now we apply the modulus to $\mathrm{rot}_{\boldsymbol{y}}\, w_q$, use a telescope sum and a triangle inequality, in order to obtain

$$\begin{aligned}|\,\mathrm{rot}_{\boldsymbol{y}}\, w_q| &\le \frac{1}{|V_{\boldsymbol{y}}|} \sum_{\sigma \in \mathcal{E}_\sigma} \frac{|\sigma^\perp|}{\sum_{\sigma' \in \mathcal{E}_{\boldsymbol{y}}} |\sigma'|} \left(\sum_{\sigma' \in \mathcal{E}_{\boldsymbol{y}}} |\sigma'| \sum_{i=1}^{|\mathcal{E}_{\boldsymbol{y}}|} \left| \bar{\boldsymbol{w}}_{\sigma_{\boldsymbol{y}}(i)} - \bar{\boldsymbol{w}}_{\sigma_{\boldsymbol{y}}(i+1)} \right| \right) \\ &= \frac{1}{|V_{\boldsymbol{y}}|} \left(\sum_{\sigma \in \mathcal{E}_\sigma} |\sigma^\perp| \right) \left(\sum_{i=1}^{|\mathcal{E}_{\boldsymbol{y}}|} \left| \bar{\boldsymbol{w}}_{\sigma_{\boldsymbol{y}}(i)} - \bar{\boldsymbol{w}}_{\sigma_{\boldsymbol{y}}(i+1)} \right| \right).\end{aligned}$$

Here, $|\boldsymbol{v}|$ for $\boldsymbol{v} \in \mathbb{R}^2$ is the Euclidean vector norm. For boundary nodes $\boldsymbol{y} \in \mathcal{V}_{\mathrm{bnd}}$ we obtain the same estimate by a similar argument accounting for the zero boundary conditions of $\boldsymbol{w}_q \in H^1_0(\Omega)^2$. Now, for all $\boldsymbol{y} \in \mathcal{V}$ we want to estimate the term

$$\begin{aligned}|V_{\boldsymbol{y}}| (\mathrm{rot}_{\boldsymbol{y}}\, w_q)^2 &\le \frac{1}{|V_{\boldsymbol{y}}|} \left(\sum_{\sigma \in \mathcal{E}_\sigma} |\sigma^\perp| \right)^2 \left(\sum_{i=1}^{|\mathcal{E}_{\boldsymbol{y}}|} \left| \bar{\boldsymbol{w}}_{\sigma_{\boldsymbol{y}}(i)} - \bar{\boldsymbol{w}}_{\sigma_{\boldsymbol{y}}(i+1)} \right| \right)^2 \\ &\le \frac{|\mathcal{E}_{\boldsymbol{y}}|}{|V_{\boldsymbol{y}}|} \left(\sum_{\sigma \in \mathcal{E}_\sigma} |\sigma^\perp| \right)^2 \sum_{i=1}^{|\mathcal{E}_{\boldsymbol{y}}|} \left| \bar{\boldsymbol{w}}_{\sigma_{\boldsymbol{y}}(i)} - \bar{\boldsymbol{w}}_{\sigma_{\boldsymbol{y}}(i+1)} \right|^2,\end{aligned}$$

where the index set $\{T_{\boldsymbol{y},i}\}$ denotes the triangles around the vertex $\boldsymbol{y}$. Using Lemma 4.4 we arrive at

$$|V_{\boldsymbol{y}}| (\mathrm{rot}_{\boldsymbol{y}}\, w_q)^2 \le C_{\mathrm{geom},1} |\mathcal{E}_{\boldsymbol{y}}| \cdot C_{\mathrm{geom},2} \sum_{i=1}^{|\mathcal{E}_{\boldsymbol{y}}|} \int_{T_{\boldsymbol{y},i}} |\nabla \boldsymbol{w}_{\boldsymbol{q}}(\boldsymbol{x})|^2 \mathrm{d}\boldsymbol{x}.$$

Last but not least, we recognize that

$$\|\mathrm{rot}_{\mathcal{V}}\, w_q\|^2_{L^2(\Omega)} \le 3 C_{\mathrm{geom}} |\mathcal{E}_{\boldsymbol{y}}|^2 \|\nabla \boldsymbol{w}_q\|^2_{L^2(\Omega)^2} \le \frac{3 C_{\mathrm{geom}} |\mathcal{E}_{\boldsymbol{y}}|^2}{\beta^2} \|q\|^2_{L^2(\Omega)}$$

holds, because every triangle has three vertices and is therefore met three times in the summation over all vertices. □

Let us now state that Problem (2.27)-(2.28)-(2.29) is well-posed.

LEMMA 4.6 (Existence and uniqueness of the discrete solution to the normal velocity scheme). *Under hypothesis* (1.5), *let* $\mathcal{M} = (\mathcal{V}, \mathcal{E}, \mathcal{T})$ *be a mesh of the domain* Ω *in the sense of Definition 2.1 and let* $\theta > 0$ *such that* $\theta_{\mathcal{M}} \geq \theta$. *Then the following inequality holds*

$$\|\mathcal{R}_{\mathcal{T}} p_{\mathcal{T}}\|_{L^2(\Omega)} \leq C \|\boldsymbol{f}\|_{L^2(\Omega)^2}, \tag{4.13}$$

where C *only depends on* θ *and* Ω. *As a consequence, there exists one and only one* $(v, p_{\mathcal{T}})$ *solution to Problem* (2.27)-(2.28)-(2.29). *Moreover,* v *is the solution of Problem* (2.31).

PROOF. We already noticed that any solution $(v, p_{\mathcal{T}})$ to Problem (2.27)-(2.28)-(2.29) is solution to Problem (2.31). Applying Lemma 4.3, we get that v is unique. Since $\int_\Omega \mathcal{R}_{\mathcal{T}} p_{\mathcal{T}}(\boldsymbol{x})\mathrm{d}\boldsymbol{x} = 0$, let $w_q \in \dot{X}_{\mathcal{E}}$ be the discrete Nečas lifting of the pressure from Lemma 4.5 satisfying

$$\begin{aligned} &\mathrm{div}_{\mathcal{T}}\, w_q = q, \\ &\|w_q\|_{X_{\mathcal{E}}^\perp} \leq C_N \|q\|_{L^2(\Omega)} \end{aligned}$$

where C_N only depends on Ω. This leads to

$$\begin{aligned} \|\mathcal{R}_{\mathcal{T}} p_{\mathcal{T}}\|_{L^2(\Omega)}^2 &= \int_\Omega \mathrm{rot}_{\mathcal{V}}\, v(\boldsymbol{x})\, \mathrm{rot}_{\mathcal{V}}\, w_q(\boldsymbol{x})\mathrm{d}\boldsymbol{x} + \int_\Omega \boldsymbol{f}(\boldsymbol{x}) \cdot \mathcal{R}_{\mathcal{E}}^\perp w_q(\boldsymbol{x})\mathrm{d}\boldsymbol{x} \\ &\leq 2CC_N \|\boldsymbol{f}\|_{L^2(\Omega)^d} \|\mathcal{R}_{\mathcal{T}} p_{\mathcal{T}}\|_{L^2(\Omega)}. \end{aligned}$$

Therefore we conclude (4.13). This inequality is then sufficient to prove the existence and uniqueness of $(v, p_{\mathcal{T}})$, solution to Problem (2.27)-(2.28)-(2.29). □

Let us now state two direct consequences of results proven in [**7**].

LEMMA 4.7. *Under hypothesis* (1.5), *let* $\boldsymbol{w} \in C_c^\infty(\Omega)^2$ *with* $\nabla \cdot \boldsymbol{w} = 0$ *be given and let* $\mathcal{M} = (\mathcal{V}, \mathcal{E}, \mathcal{T})$ *be a given discretization in the sense of Definition 2.1. Then there exists a quasi-interpolation operator* $\hat{\mathcal{I}}_{\mathcal{M}}^\perp : C_c^\infty(\Omega)^2 \to V_{\mathcal{E}}^\perp$ *such that*

$$\begin{aligned} \|\hat{\mathcal{R}}_{\mathcal{V}} \hat{\mathcal{I}}_{\mathcal{M}}^\perp \boldsymbol{w} - \boldsymbol{w}\|_{L^2(\Omega)^2} &\leq C_{\boldsymbol{w}} h_{\mathcal{M}} \\ \|\mathrm{rot}_{\mathcal{V}}\, \hat{\mathcal{I}}_{\mathcal{M}}^\perp \boldsymbol{w} - \mathrm{rot}\, \boldsymbol{w}\|_{L^2(\Omega)} &\leq C_{\boldsymbol{w}} h_{\mathcal{M}}, \end{aligned}$$

where $C_{\boldsymbol{w}}$ *only depends on* $\boldsymbol{w}$ *and on any* $\theta > 0$ *such that* $\theta \leq \theta_{\mathcal{M}}$. *Moreover,* $\mathcal{R}_{\mathcal{E}}^\perp \hat{\mathcal{I}}_{\mathcal{M}}^\perp \boldsymbol{w}$ *converges weakly to* $\boldsymbol{w}$ *in* $L^2(\Omega)^2$ *as* $h_{\mathcal{M}} \to 0$ *under the condition* $\theta \leq \theta_{\mathcal{M}}$.

PROOF. Similar to the tangential velocity scheme, it again suffices to consider the discrete stream function defined by Lemma 3.3 of [**6**], for getting the second inequality, and to use the result on the strong discrete reconstruction of the gradient of the discrete stream function, provided in [**5**]. □

We prove weak compactness for discretely divergence-free velocities, with bounded discrete rotation.

LEMMA 4.8. *Under hypothesis* (1.5), *let* $(\mathcal{M}_n)_{n\in\mathbb{N}}$ *be a sequence such that:*

- $\mathcal{M}_n = (\mathcal{V}_n, \mathcal{E}_n, \mathcal{T}_n)$ *is a discretization in the sense of Definition 2.1,*
- $h_{\mathcal{M}_n}$ *tends to 0 as* n *tends to* ∞ *and* $\theta_{\mathcal{M}_n} \geq \theta > 0$,
- *for all* $n \in \mathbb{N}$, *there exists* $(v_n, p_n) \in V_{\mathcal{E}_n}^\perp \times X_{\mathcal{T}_n}$ *with* $\int_\Omega \mathcal{R}_{\mathcal{T}_n} p_n \mathrm{d}\boldsymbol{x} = 0$, *such that there exists* $C > 0$, *independent of* n, *with* $\|v_n\|_{X_{\mathcal{E}_n}^\perp} = \|\mathrm{rot}_{\mathcal{V}_n}\, v_n\|_{L^2(\Omega)} \leq C$ *and* $\|\mathcal{R}_{\mathcal{T}_n} p_n\|_{L^2(\Omega)} \leq C$.

Then there exists $(\boldsymbol{v}, p) \in H_0^1(\Omega)^2 \times L_0^2(\Omega)$ *with* $\nabla \cdot \boldsymbol{v} = 0$ *and a subsequence of* $(\mathcal{M}_n)_{n\in\mathbb{N}}$, *again denoted by* $(\mathcal{M}_n)_{n\in\mathbb{N}}$, *such that*

- $\mathrm{rot}_{\mathcal{V}_n}\, v_n \rightharpoonup \mathrm{rot}\, \boldsymbol{v}$ *weakly in* $L^2(\Omega)$,
- $\mathcal{R}_{\mathcal{E}_n}^\perp v_n \rightharpoonup \boldsymbol{v}$ *weakly in* $L^2(\Omega)^2$,
- $\hat{\mathcal{R}}_{\mathcal{V}_n} v_n \longrightarrow \boldsymbol{v}$ *strongly in* $L^2(\Omega)^2$,
- $\mathcal{R}_{\mathcal{T}_n} p_n \rightharpoonup p$ *weakly in* $L^2(\Omega)$.

PROOF. Concerning the convergence of the discrete velocities, the proof of this lemma is obtained by using the discrete stream function given by Lemma 4.2, and then to apply Lemma 3.2 of [**6**]. The weak convergence of the pressure in the above sense is obvious. □

Before we state the convergence theorem, we introduce now another quasi-interpolation operator, which is needed for the proof of the convergence of the pressure.

LEMMA 4.9. *Under hypothesis* (1.5), *let* $(\mathcal{M}_n)_{n\in\mathbb{N}}$ *be a sequence such that*

- $\mathcal{M}_n = (\mathcal{V}_n, \mathcal{E}_n, \mathcal{T}_n)$ *is a discretization in the sense of Definition 2.1,*
- $h_{\mathcal{M}_n}$ *tends to 0 as* n *tends to* ∞ *and* $\theta_{\mathcal{M}_n} \geq \theta > 0$.

Then, we can construct a quasi-interpolation operator $\hat{J}^{\perp}_{\mathcal{M}_n} : H^1_0(\Omega)^2 \to \dot{X}_{\mathcal{E}_n}$, *fulfilling, for any* $\boldsymbol{w} \in H^1_0(\Omega)^2$, *that*

- *the weak reconstruction* $\mathcal{R}^{\perp}_{\mathcal{E}} \hat{J}^{\perp}_{\mathcal{M}_n} \boldsymbol{w}$ *converges weakly in* $L^2(\Omega)^2$ *to* $\boldsymbol{w}$,
- *the strong reconstruction* $\hat{\mathcal{R}}_{\mathcal{V}} \hat{J}^{\perp}_{\mathcal{M}_n} \boldsymbol{w}$ *converges strongly in* $L^2(\Omega)^2$ *to* $\boldsymbol{w}$,
- *the discrete divergence of* $\hat{J}^{\perp}_{\mathcal{M}_n} \boldsymbol{w}$ *converges strongly in* $L^2(\Omega)$ *to* $\nabla \cdot \boldsymbol{w}$,
- *the discrete rotation of* $\hat{J}^{\perp}_{\mathcal{M}_n} \boldsymbol{w}$ *converges weakly in* $L^2(\Omega)$ *to* $\operatorname{rot} \boldsymbol{w}$.

PROOF. The operator can be constructed by computing the following averages of the trace of $\boldsymbol{w}$ (also denoted for simplicity by $\boldsymbol{w}$) on the faces

$$\left(\hat{J}^{\perp}_{\mathcal{M}_n} \boldsymbol{w}\right)_{\sigma} := \frac{1}{|\sigma|} \int_{\sigma} \boldsymbol{w} \cdot \boldsymbol{n}_{\sigma} \mathrm{d}\gamma(\boldsymbol{x}),$$

for all edges $\sigma \in \mathcal{E}$. Obviously, we have the strong convergence of the divergence by the Gauss theorem. □

Eventually, we can show now the desired convergence of the scheme:

THEOREM 4.10. *Under hypothesis* (1.5), *let* $(\mathcal{M}_n)_{n\in\mathbb{N}}$ *be a sequence such that*

- $\mathcal{M}_n = (\mathcal{V}_n, \mathcal{E}_n, \mathcal{T}_n)$ *is a discretization in the sense of Definition 2.1,*
- $h_{\mathcal{M}_n}$ *tends to 0 as* n *tends to* ∞ *and* $\theta_{\mathcal{M}_n} \geq \theta > 0$,

and let $\boldsymbol{f} \in L^2(\Omega)^2$. *Then, for every* $n \in \mathbb{N}$ *there exists one and only one* $(v_n, p_n) \in V^{\perp}_{\mathcal{E}_n} \times X_{\mathcal{T}_n}$ *such that* (2.20)-(2.21)-(2.22) *hold. Moreover, assuming that* $h_{\mathcal{M}}$ *tends to* 0 *while* $\theta_{\mathcal{M}} \geq \theta$ *for some* $\theta > 0$, *then, denoting by* $(\boldsymbol{v}, p) \in H^1_0(\Omega)^2 \times L^2_0(\Omega)$ *the weak solution of Problem* (1.1)-(1.4), *we have convergence in the following sense*

- $\operatorname{rot}_{\mathcal{V}_n} v_n \longrightarrow \operatorname{rot} \boldsymbol{v}$ *in* $L^2(\Omega)$,
- $\mathcal{R}^{\perp}_{\mathcal{E}_n} v_n \rightharpoonup \boldsymbol{v}$ *weakly in* $L^2(\Omega)^2$,
- $\hat{\mathcal{R}}_{\mathcal{V}_n} v_n \longrightarrow \boldsymbol{v}$ *in* $L^2(\Omega)^2$.
- $\mathcal{R}_{\mathcal{T}_n} p_n \longrightarrow p$ *in* $L^2(\Omega)$.

PROOF. Let us first write an a-priori estimate on the approximate solution. We let $w = v$ in (2.31). We get

$$\int_{\Omega} (\operatorname{rot}_{\mathcal{V}_n} v_n)^2 \mathrm{d}\boldsymbol{x} = \int_{\Omega} \boldsymbol{f} \cdot \mathcal{R}^{\perp}_{\mathcal{E}_n} v_n \mathrm{d}\boldsymbol{x}. \tag{4.14}$$

We now apply the Cauchy-Schwarz inequality to the right hand side of the above equation. We get

$$\|v_n\|^2_{X^{\perp}_{\mathcal{E}_n}} \leq \|\boldsymbol{f}\|_{L^2(\Omega)^2} \|\mathcal{R}^{\perp}_{\mathcal{E}_n} v_n\|_{L^2(\Omega)^2} \leq C_1 \|\boldsymbol{f}\|_{L^2(\Omega)^2} \|v\|_{X^{\perp}_{\mathcal{E}_n}}.$$

This provides

$$\|v_n\|_{X^{\perp}_{\mathcal{E}_n}} \leq C_1 \|\boldsymbol{f}\|_{L^2(\Omega)^2},$$

which shows that scheme (2.31), which leads to a square linear system whose unknowns are the degrees of freedom in vector space $V_{\mathcal{E}_n}$, has one and only one solution. Indeed, it suffices to take $\boldsymbol{f} = 0$; then the previous inequality shows that $v_n = 0$. We now remark that the previous inequality allows to apply Lemma 4.8. Therefore, taking a sequence of discretizations $(\mathcal{M}_n)_{n\in\mathbb{N}}$ such that $h_{\mathcal{M}_n}$ tends to 0 as n tends to ∞ and $\theta_{\mathcal{M}_n} \geq \theta > 0$, we get the existence of a subsequence (denoted by the same notation) and of $\boldsymbol{v} \in H^1_0(\Omega)^2$ such that the conclusions of Lemma 4.8 hold.

Let $\boldsymbol{w} \in C^{\infty}_c(\Omega)^2$ with $\nabla \cdot \boldsymbol{w}$ be given, and let us apply the above quasi-interpolation operator $\hat{\mathcal{I}}^{\perp}_{\mathcal{M}_n} \boldsymbol{w} \in V^{\perp}_{\mathcal{E}}$ in (2.20). We get

$$\int_{\Omega} \operatorname{rot}_{\mathcal{V}_n} v_n \operatorname{rot}_{\mathcal{V}_n} \hat{\mathcal{I}}^{\perp}_{\mathcal{M}_n} \boldsymbol{w} \mathrm{d}\boldsymbol{x} = \int_{\Omega} \boldsymbol{f} \cdot \mathcal{R}^{\perp}_{\mathcal{E}_n} \hat{\mathcal{I}}^{\perp}_{\mathcal{M}_n} \boldsymbol{w} \mathrm{d}\boldsymbol{x}.$$

Thanks to Lemmas 4.7 and 4.8, we may pass to the limit $n \to \infty$ in the above equation, since the use of both lemmas provides standard weak/strong convergence in the left hand side. We then get

$$\int_\Omega \operatorname{rot} \boldsymbol{v} \operatorname{rot} \boldsymbol{w} \mathrm{d}\boldsymbol{x} = \int_\Omega \boldsymbol{f} \cdot \boldsymbol{w} \mathrm{d}\boldsymbol{x}. \tag{4.15}$$

According to a density theorem given by Temam [**26**], the smooth divergence-free functions functions are dense in the set of all divergence-free $H_0^1(\Omega)^2$ functions, which proves that $\boldsymbol{v}$ is the unique weak solution of Problem (1.1)-(1.4). A standard reasoning then shows that the entire sequence converges, which leads to the convergence of the scheme. Let us now prove the convergence of $\operatorname{rot}_{\mathcal{V}_n} v_n$ to $\operatorname{rot} \boldsymbol{v}$ in $L^2(\Omega)$. Passing to the limit in (2.31), with $v = w = v_n$, we get that the limit of $\|v_n\|^2_{X_{\mathcal{E}_n}^\perp}$ is equal to $\int_\Omega \boldsymbol{f} \cdot \boldsymbol{v} \mathrm{d}\boldsymbol{x} = \|\operatorname{rot} \boldsymbol{v}\|^2_{L^2(\Omega)}$. This, in addition to the weak convergence result given by Lemma 4.8, proves the strong convergence of $\operatorname{rot}_{\mathcal{V}} v_n$.

Turning now to the strong convergence of the reconstructed pressure, we first note that due to the inequality (4.13) and Lemma 4.8 we have weak convergence of the discrete pressures $\mathcal{R}_{\mathcal{T}_n} p_n$ in $L^2(\Omega)$ to some $q \in L^2_0(\Omega)$. In order to show that this pressure is indeed the solution of the continuous Stokes problem, we first apply the above quasi-interpolation operator from Lemma 4.9 to any $\boldsymbol{w} \in C_c^\infty(\Omega)^2$. Using the discrete test function $\hat{J}^\perp_{\mathcal{M}_n} \boldsymbol{w}$, there holds according to (2.27):

$$\int_\Omega \mathcal{R}_{\mathcal{T}_n} p_n \operatorname{div}_{\mathcal{T}_n} \hat{J}^\perp_{\mathcal{M}_n} \boldsymbol{w} \mathrm{d}\boldsymbol{x} = \int_\Omega \operatorname{rot}_{\mathcal{V}_n} v_n \operatorname{rot}_{\mathcal{V}_n} \hat{J}^\perp_{\mathcal{M}_n} \boldsymbol{w} \mathrm{d}\boldsymbol{x} - \int_\Omega \boldsymbol{f} \cdot \mathcal{R}^\perp_{\mathcal{E}_n} \hat{J}^\perp_{\mathcal{M}_n} \boldsymbol{w} \mathrm{d}\boldsymbol{x}.$$

In the first term we get, thanks to weak/strong convergence,

$$\lim_{n\to\infty} \int_\Omega \mathcal{R}_{\mathcal{T}_n} p_n \operatorname{div}_{\mathcal{T}_n} \hat{J}^\perp_{\mathcal{M}_n} \boldsymbol{w} \mathrm{d}\boldsymbol{x} = \int_\Omega q \nabla \cdot \boldsymbol{w} \mathrm{d}\boldsymbol{x},$$

using strong convergence property for $\operatorname{div}_{\mathcal{T}_n} \hat{J}^\perp_{\mathcal{M}_n} \boldsymbol{w}$. In the third term we get, thanks to weak convergence,

$$\lim_{n\to\infty} \int_\Omega \boldsymbol{f} \cdot \mathcal{R}^\perp_{\mathcal{E}_n} \hat{J}^\perp_{\mathcal{M}_n} \boldsymbol{w} \mathrm{d}\boldsymbol{x} = \int_\Omega \boldsymbol{f} \cdot \boldsymbol{w} \mathrm{d}\boldsymbol{x}.$$

Also in the second term we again get, using weak/strong convergence,

$$\lim_{n\to\infty} \int_\Omega \operatorname{rot}_{\mathcal{V}_n} v_n \operatorname{rot}_{\mathcal{V}_n} \hat{J}^\perp_{\mathcal{M}_n} \boldsymbol{w} \mathrm{d}\boldsymbol{x} = \int_\Omega \operatorname{rot} \boldsymbol{v} \operatorname{rot} \boldsymbol{w} \mathrm{d}\boldsymbol{x},$$

(recall that we only obtain a weak convergence property for $\operatorname{rot}_{\mathcal{V}_n} \hat{J}^\perp_{\mathcal{M}_n} \boldsymbol{w}$, but we have previously proved the strong convergence of $\operatorname{rot}_{\mathcal{V}_n} v_n$). Therefore, the pressure q is indeed the pressure solution p of the continuous Stokes equations.

Let us now show that $\mathcal{R}_{\mathcal{T}_n} p_n$ also strongly converges in L^2. To this aim, we use a sequence of continuous Nečas liftings $\boldsymbol{q}_n \in H_0^1(\Omega)^2$ such that $\nabla \cdot \boldsymbol{q}_n = p_n$ holds, and we define from these continuous liftings the corresponding discrete Nečas liftings $w_n = \hat{J}^\perp_{\mathcal{M}_n} \boldsymbol{q}_n$. For the continuous Nečas liftings we extract a subsequence such that we can use Rellich's theorem, and we may pass to the limit $n \to \infty$ (thanks to the strong convergence result on $\operatorname{rot}_{\mathcal{T}_n} v_n$ and to the weak convergence of $\operatorname{rot}_{\mathcal{T}_n} w_n$ to $\operatorname{rot} \boldsymbol{q}$). We then get

$$\int_\Omega \operatorname{rot} \boldsymbol{v} \operatorname{rot} \boldsymbol{q} \mathrm{d}\boldsymbol{x} - \lim_{n\to\infty} \int_\Omega (\mathcal{R}_{\mathcal{T}_n} p_n)^2 \mathrm{d}\boldsymbol{x} = \int_\Omega \boldsymbol{f} \cdot \boldsymbol{q} \mathrm{d}\boldsymbol{x}.$$

Since $\nabla \cdot \boldsymbol{q} = p$, we get, introducing $\boldsymbol{q}$ as test function that

$$\lim_{n\to\infty} \int_\Omega (\mathcal{R}_{\mathcal{T}_n} p)^2 \mathrm{d}\boldsymbol{x} = \int_\Omega p^2 \mathrm{d}\boldsymbol{x},$$

hence showing the strong convergence of the pressure in $L^2(\Omega)$. □

5. The Navier-Stokes problem

In this section, all the considerations hold for both the tangential and the normal velocity scheme. Therefore we introduce the following unifying notations: Let $\mathcal{M} = (\mathcal{V}, \mathcal{E}, \mathcal{T})$ be a discretization in the sense of Definition 2.1. For the tangential velocity scheme, we write $\mathcal{R}_\mathcal{E} := \mathcal{R}^\parallel_\mathcal{E}, \hat{\mathcal{R}}_\mathcal{M} := \hat{\mathcal{R}}_\mathcal{T}, \mathrm{rot}_\mathcal{M} := \mathrm{rot}_\mathcal{T}, \mathcal{V}_\mathcal{E} := \mathcal{V}^\parallel_\mathcal{E}, \mathcal{I}_\mathcal{M} := \mathcal{I}^\parallel_\mathcal{M}$. In the case of the normal velocity scheme, we use $\mathcal{R}_\mathcal{E} := \mathcal{R}^\perp_\mathcal{E}, \hat{\mathcal{R}}_\mathcal{M} := \hat{\mathcal{R}}_\mathcal{V}, \mathrm{rot}_\mathcal{M} := \mathrm{rot}_\mathcal{V}, \mathcal{V}_\mathcal{E} := \mathcal{V}^\perp_\mathcal{E}, \mathcal{I}_\mathcal{M} := \mathcal{I}^\perp_\mathcal{M}$.

We now consider the Navier-Stokes problem, which can be formulated as: find $\boldsymbol{v} \in H^1_0(\Omega)^2$ with $\mathrm{div}\,\boldsymbol{v} = 0$ and

$$\int_\Omega \mathrm{rot}\,\boldsymbol{v}\,\mathrm{rot}\,\boldsymbol{w}\mathrm{d}\boldsymbol{x} + \int_\Omega \mathrm{rot}\,\boldsymbol{v}(v^{(1)}w^{(2)} - v^{(2)}w^{(1)})\mathrm{d}\boldsymbol{x} = \int_\Omega \boldsymbol{f}\cdot\boldsymbol{w}\mathrm{d}\boldsymbol{x},$$
$$\forall \boldsymbol{w} \in H^1_0(\Omega)^2 \text{ with } \mathrm{div}\,\boldsymbol{w} = 0. \tag{5.1}$$

We consider the following numerical scheme: find $v \in V_\mathcal{E}$ such that

$$\int_\Omega \mathrm{rot}_\mathcal{M}\, v\,\mathrm{rot}_\mathcal{M}\, w\mathrm{d}\boldsymbol{x} + \int_\Omega \mathrm{rot}_\mathcal{M}\, v\ (\hat{\mathcal{R}}^{(1)}_\mathcal{M} v \hat{\mathcal{R}}^{(2)}_\mathcal{M} w - \hat{\mathcal{R}}^{(2)}_\mathcal{M} v \hat{\mathcal{R}}^{(1)}_\mathcal{M} w)\mathrm{d}\boldsymbol{x}$$
$$= \int_\Omega \boldsymbol{f}\cdot\mathcal{R}_\mathcal{E} w\mathrm{d}\boldsymbol{x},\ \forall w \in V_\mathcal{E}. \tag{5.2}$$

We then have the following result.

Theorem 5.1. *Let $(\mathcal{M}_n)_{n\in\mathbb{N}}$ be a sequence such that:*

- *$\mathcal{M}_n = (\mathcal{V}_n, \mathcal{E}_n, \mathcal{T}_n)$ is a discretization in the sense of Definition 2.1,*
- *$h_{\mathcal{M}_n}$ tends to 0 as n tends to ∞ and $\theta_{\mathcal{M}_n} \geq \theta > 0$.*

Then, for all $n \in \mathbb{N}$, there exists at least one $v_n \in V_{\mathcal{E}_n}$ such that (5.2) holds, and there exists $\boldsymbol{v} \in H^1_0(\Omega)^2$ and a subsequence of $(\mathcal{M}_n)_{n\in\mathbb{N}}$, again denoted by $(\mathcal{M}_n)_{n\in\mathbb{N}}$, such that

- *$\boldsymbol{v}$ is a solution to (5.1),*
- *$\mathrm{rot}_{\mathcal{M}_n} v_n \longrightarrow \mathrm{rot}\,\boldsymbol{v}$ in $L^2(\Omega)$,*
- *$\mathcal{R}_{\mathcal{E}_n} v_n \rightharpoonup \boldsymbol{v}$ weakly in $L^2(\Omega)^2$,*
- *$\hat{\mathcal{R}}_{\mathcal{M}_n} v_n \longrightarrow \boldsymbol{v}$ in $L^2(\Omega)^2$.*

Proof. In order to show the existence of a discrete solution, we consider the function $\Psi : V_\mathcal{E} \to V_\mathcal{E}$, such that $v = \Psi(\widetilde{v})$ is the solution of

$$\int_\Omega \mathrm{rot}_\mathcal{M}\, v\,\mathrm{rot}_\mathcal{M}\, w\mathrm{d}\boldsymbol{x} + \int_\Omega \mathrm{rot}_\mathcal{M}\, \widetilde{v}\ (\hat{\mathcal{R}}^{(1)}_\mathcal{M} v \hat{\mathcal{R}}^{(2)}_\mathcal{M} w - \hat{\mathcal{R}}^{(2)}_\mathcal{M} v \hat{\mathcal{R}}^{(1)}_\mathcal{M} w)\mathrm{d}\boldsymbol{x}$$
$$= \int_\Omega \boldsymbol{f}\cdot\mathcal{R}_\mathcal{E} w\mathrm{d}\boldsymbol{x},\ \forall w \in V_\mathcal{E}.$$

Indeed, we prove, setting $w = v$, since the term containing $\widetilde{v}$ vanishes, that

$$\|v\|_{X_\mathcal{E}} \leq C_1 \|\boldsymbol{f}\|_{L^2(\Omega)^2}. \tag{5.3}$$

Hence the function Ψ is uniquely defined, it is continuous, and maps a bounded ball into itself. Hence, thanks to Brouwer's theorem, it admits a fixed point, which proves that the scheme has at least one solution. This solution satisfies the estimate (5.3), which allows to apply, as in the linear case, the compactness Lemma 3.5. Hence, for $\boldsymbol{w} \in C^\infty_c(\Omega)^2$ with $\nabla\cdot\boldsymbol{w} = 0$, considering the provided subsequence, we pass to the limit on the scheme setting $w = \hat{\mathcal{I}}_{\mathcal{M}_n}\boldsymbol{w} \in V_\mathcal{E}$. Remark that, at this time, we only know that $\mathrm{rot}_{\mathcal{M}_n} v_n$ converges weakly to $\mathrm{rot}\,\boldsymbol{v}$ in $L^2(\Omega)$. Nevertheless, this is sufficient to write that the term

$$\int_\Omega \mathrm{rot}_{\mathcal{M}_n}\, v_n\ (\hat{\mathcal{R}}^{(1)}_{\mathcal{M}_n} v_n \hat{\mathcal{R}}^{(2)}_{\mathcal{M}_n} \hat{\mathcal{I}}_{\mathcal{M}_n}\boldsymbol{w} - \hat{\mathcal{R}}^{(2)}_{\mathcal{M}_n} v \hat{\mathcal{R}}^{(1)}_{\mathcal{M}_n} \hat{\mathcal{I}}_{\mathcal{M}_n}\boldsymbol{w})\mathrm{d}\boldsymbol{x}$$

converges to

$$\int_\Omega \mathrm{rot}\,\boldsymbol{v}(v^{(1)}w^{(2)} - v^{(2)}w^{(1)})\mathrm{d}\boldsymbol{x}.$$

Therefore we get that $\boldsymbol{v}$ is a solution to (5.1), and by setting $\boldsymbol{w} = \boldsymbol{v}$, that $\int_\Omega \boldsymbol{f}\cdot\boldsymbol{v}\mathrm{d}\boldsymbol{x} = \|\mathrm{rot}\,\boldsymbol{v}\|^2_{L^2(\Omega)}$. Setting $w = v$ in the scheme, we get as in the linear case that the limit of $\|v_n\|^2_{X_{\mathcal{E}_n}}$ is equal to $\int_\Omega \boldsymbol{f}\cdot\boldsymbol{v}\mathrm{d}\boldsymbol{x} = \|\mathrm{rot}\,\boldsymbol{v}\|^2_{L^2(\Omega)}$, which proves the strong convergence of $\mathrm{rot}_{\mathcal{M}_n} v_n$ to $\mathrm{rot}\,\boldsymbol{v}$ in $L^2(\Omega)$. □

6. Numerical results

6.1. Linear example. In order to investigate numerically the convergence rate that can be achieved with the extended MAC scheme above, we compute an academic Stokes problem on two sequences of meshes. We remark that we achieved the same experimental convergence rates for the full nonlinear Navier-Stokes equations. The problem is posed on $\Omega = [0,1]^2$, has homogeneous Dirichlet boundary conditions and reads

$$\begin{aligned}\xi &= x^2(x-1)^2y^2(y-1)^2,\\ \boldsymbol{v} &= \begin{pmatrix} 2(x-1)^2x^2(y-1)y(2y-1)\\ -2(2x-1)(x-1)x(y-1)^2y^2\end{pmatrix},\\ p &= x^3+y^3-\frac{1}{2}.\end{aligned}$$

The force vector $\boldsymbol{f}$ is computed such that $\boldsymbol{v}$ and p fulfill the incompressible Stokes equations.

In the first sequence of meshes, every mesh is built up from small squares, where the side length of such a square defines the mesh size. Every square in the mesh is split into two triangles. Then, the mesh is not admissible in the strict sense of the above definition, since the circumcenters of these two triangles coincide. But this does not pose any problem, since in this degenerated case, the discrete method is equivalent to a method where the squares take over the role of triangles, and the diagonals of the squares can be removed from the above considerations. Indeed, the measure of their corresponding Voronoi faces are zero. At the same time, on these meshes, triangle edge midpoints and Voronoi face midpoints coincide. This fact will result in superior convergence behavior on these meshes in comparison to "purely" triangular meshes.

In Table 1 we show some information about the degrees of freedom in these square meshes. The last two columns of this table show some quite interesting information. The penultimate column reveals that the tangential velocity scheme is quite efficient in terms of degrees of freedom, since the ratio between the number of degrees of freedom corresponding to discretely divergence-free velocities and the total number of degrees of freedom is about 0.5. For the normal velocity scheme, the corresponding ratio is only 0.20.

mesh size	$\lvert E\rvert$	$\lvert V\rvert$	$\lvert T\rvert$	$\frac{\lvert E\rvert-\lvert V\rvert}{\lvert E\rvert+\lvert V\rvert}$	$\frac{\lvert E\rvert-\lvert T\rvert}{\lvert E\rvert+\lvert T\rvert}$
$\frac{1}{32}$	2945	1024	1922	0.484	0.210
$\frac{1}{64}$	12033	4096	7938	0.492	0.205
$\frac{1}{128}$	48641	16384	32258	0.496	0.203
$\frac{1}{256}$	195585	65536	130050	0.498	0.201
$\frac{1}{512}$	784385	262144	522242	0.499	0.201
$\frac{1}{1024}$	3141633	1048576	2093058	0.500	0.200

TABLE 1. Number of edges, vertices and triangles in different square meshes. The penultimate column shows the ratio between discretely divergence-free degrees of freedom and the total number of degrees of freedom for the tangential velocity scheme. The last column shows the ratio between discretely divergence-free degrees of freedom and the total number of degrees of freedom for the normal velocity scheme.

The second sequence of meshes are made up of isotropic, unstructured boundary conforming Delaunay meshes. They have been generated by the mesh generator TRIANGLE [**24**]. We remark, that this approach does not guarantee that the triangulation is acute. In Table 2 we show some information about the degrees of freedom in these triangle meshes. An approximate mesh size was defined according to the largest triangle area that the mesh generator was allowed to generate within a mesh. From Tables 1 and 2 we recognize that the degrees of freedom of corresponding meshes in the two mesh families are quite similar, such that the definition of the mesh size for unstructured meshes seems to be reasonable.

The two schemes are implemented within the framework of the software package PDELIB2 [**8**]. All the discrete linear systems are solved with the direct solver PARDISO [**22, 23**].

mesh size	$\|E\|$	$\|V\|$	$\|T\|$	$\frac{\|E\|-\|V\|}{\|E\|+\|V\|}$	$\frac{\|E\|-\|T\|}{\|E\|+\|T\|}$
$\frac{1}{32}$	3121	1084	2038	0.484	0.210
$\frac{1}{64}$	12326	4195	8132	0.492	0.205
$\frac{1}{128}$	48664	16393	32272	0.496	0.203
$\frac{1}{256}$	194879	65302	129578	0.498	0.201
$\frac{1}{512}$	779506	260519	518988	0.499	0.201
$\frac{1}{1024}$	3114404	1039501	2074904	0.500	0.200

TABLE 2. Number of edges, vertices and triangles in different Delaunay meshes generated by the mesh generator TRIANGLE [**24**]. The penultimate column shows the ratio between discretely divergence-free degrees of freedom and the total number of degrees of freedom for the tangential velocity scheme. The last column shows the ratio between discretely divergence-free degrees of freedom and the total number of degrees of freedom for the normal velocity scheme.

In Figures 4 and 5, for both schemes and series of meshes, we plot various measures of the error between the discrete solution and a projection of the exact solution onto the grid. We used two different projections for both schemes. For the tangential velocity scheme, we evaluate the tangential velocities at the edge midpoints and assign them to the corresponding velocity degrees of freedom. For the normal velocity scheme, we evaluate the normal velocities at the Voronoi face midpoints and assign them to the corresponding velocity degrees of freedom, likewise.

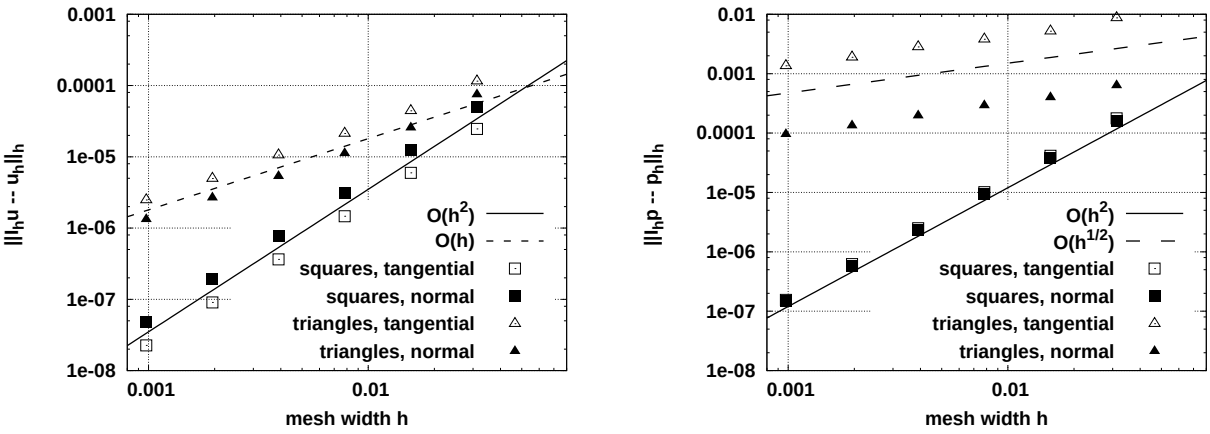

FIGURE 4. Discrete L^2-norm of the error between the projected exact solution and the discrete solution. Left: velocity, right: pressure.

We start the discussion with the approximation of the velocity, see Fig. 4, left. We observe similar behavior for the two discretization schemes proposed. On triangular meshes the convergence order is approximately $O(h)$. On square meshes, we gain an order of magnitude in the convergence rate in comparison to the triangular meshes.

Also, concerning the approximation orders of the pressure, both schemes behave in a similar way, including second order convergence on square meshes, see Fig. 4, right. We observe that on triangular meshes, the convergence order drops to $O(h^{\frac{1}{2}})$. At the same time, the accuracy of the normal velocity scheme on triangular meshes is better by a factor of ≈ 10 in comparison to the tangential velocity scheme.

The discrete rotation is convergent for both schemes. This is confirmed by Fig. 5 (left), where we observe the convergence of the difference between the discrete rotation of the discrete solution and the discrete rotation of the projected exact solution. On square meshes, for the normal velocity scheme, the L^2 norm of this difference exhibits $O(h^{\frac{3}{2}})$-convergence, while the convergence order of the tangential velocity scheme is only $O(h)$. On triangular meshes, both schemes exhibit $O(h^{\frac{1}{2}})$ convergence with an advantage for the normal velocity scheme concerning the constants.

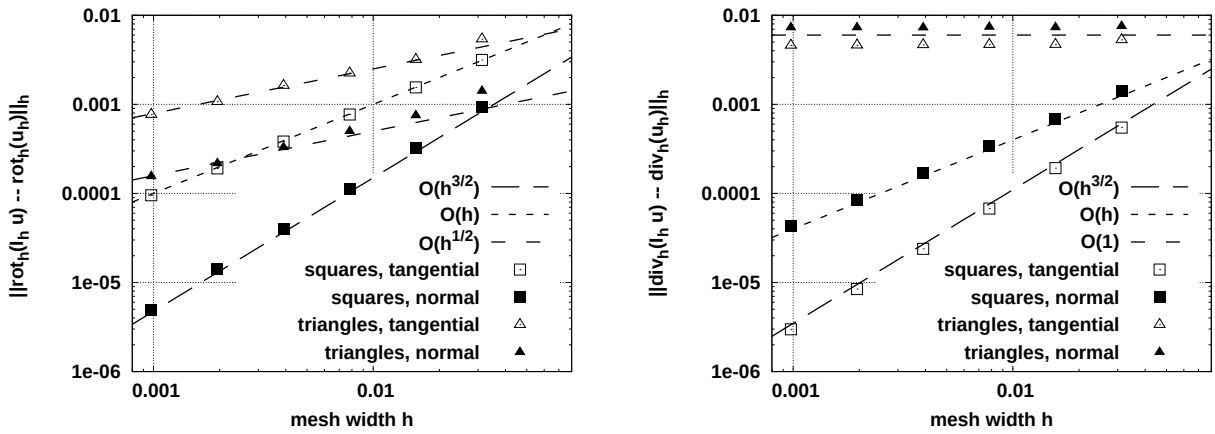

FIGURE 5. Discrete L^2-norm of the discrete vector calculus operators applied to the difference between the projected exact velocity and the velocity component of the discrete solution. Left: rotational, right: divergence.

By construction, for both schemes, the discrete divergence of the velocity component of the discrete solution is zero. Therefore, the error shown in Fig. 5 (right) coincides with the discrete divergence of the projected exact velocity. On square meshes, for both schemes, the discrete divergence operator is consistent, since midpoints of an edge coincide with midpoints of the orthogonal Voronoi faces. Therefore, the discrete divergence converges on square meshes to zero with order $O(h^{1.5})$ for the tangential velocity scheme and $O(h)$ for the normal velocity scheme. On the triangular meshes, edge midpoints and Voronoi face midpoints do not coincide and the discrete divergence operator is not consistent resulting in no convergence at all if it is applied to the projection of the velocity component of the exact solution.

We note that the convergence behavior on the boundary conforming Delaunay meshes, which are not acute, is consistent with the theoretical considerations which for technical reasons had been constrained to acute triangulations.

6.2. Nonlinear driven cavity. Besides delivering experimental orders of convergence for some academic flow problem, we want to show that the presented generalized MAC scheme can indeed solve non-trivial nonlinear flow problems. The following results are produced by the tangential velocity scheme.

6.2.1. *Driven cavity in a square.* First, we show results for a driven cavity problem in a square [**11**] with $\Omega = [0,1]^2$, inhomogeneous Dirichlet boundary conditions and a right hand side $\boldsymbol{f} = \boldsymbol{0}$. The inhomogeneous Dirichlet boundary conditions are given by $\boldsymbol{v} = (1,0)^T$ for $\boldsymbol{x} \in [0,1] \times \{1\}$ and $\boldsymbol{v} = \boldsymbol{0}$ for $\partial\Omega \setminus [0,1] \times \{1\}$. This problem does not fit into our framework in the strict sense, since due to the discontinuous Dirichlet boundary conditions, the solution of this driven cavity problem is not contained in the Sobolev space $H^1(\Omega)^2$.

We used an unstructured Delaunay triangulation generated by the mesh generator TRIANGLE [**24**]. We emphasize that though the driven cavity problem can be simulated by the classical MAC scheme, it would not be possible to use an unstructured grid for this. As a result, we confirm that the generalized MAC scheme is indeed much more flexible than the classical one.

We solve the problem at the rather moderate Reynolds number 400 using a Picard iteration to resolve the nonlinearity. On a mesh with 16,028 vertices we needed 69 iteration steps to reduce the nonlinear residual to the size of the residual of the direct solver PARDISO [**22, 23**].

We recover the classical results for this problem [**11**], i.e., the flow is made up from three vortices, a large central vortex, a smaller vortex in the right bottom corner, and finally an even smaller vortex in the left bottom corner, see Figures 6 and 7.

For higher Reynolds numbers like 1,000, it was very difficult to solve the nonlinear system. This problem is well-known for the rotational form of the Navier-Stokes equations, and may be attributed to the complex structure of the Bernoulli pressure [**1**].

6.2.2. *Driven cavity in an equilateral triangle.* Our last numerical example, the driven cavity flow in the equilateral triangle with corners $(0,1)^T$, $(1,1)^T$ $(\frac{1}{2}, 1 - \frac{\sqrt{3}}{2})^T$ [**3**], demonstrates that the generalized MAC scheme allows to compute flows in geometries which cannot be handled well by the

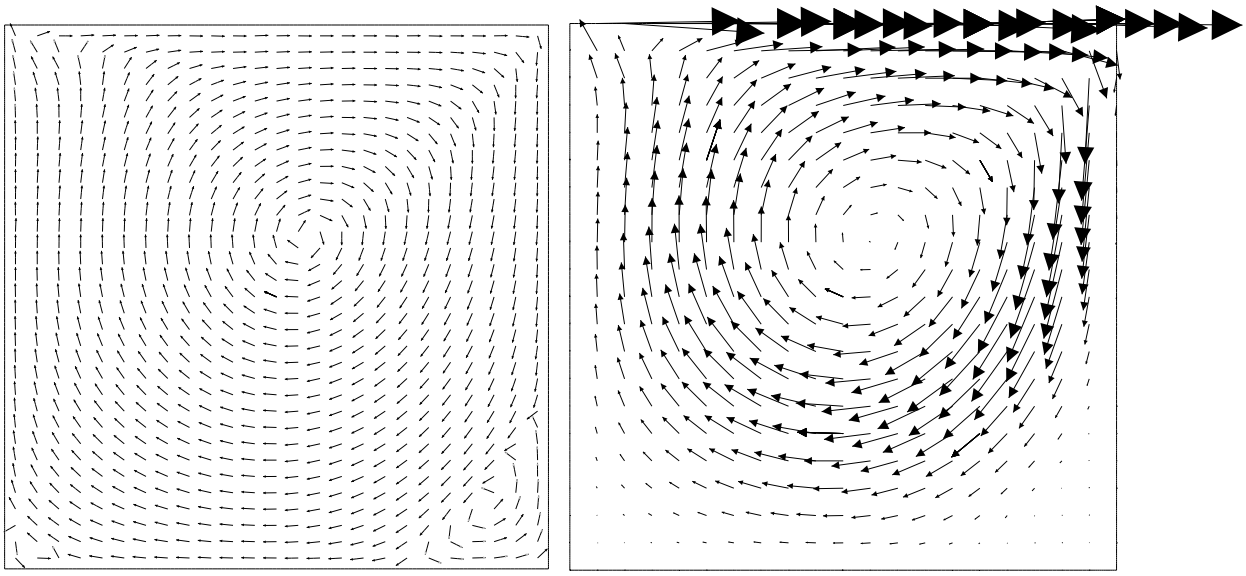

FIGURE 6. Driven cavity in a square, Reynolds number 400. Left: the equal length arrows show the interpolated velocity directions on a coarse raster. The three vortices in the central part of the cavity, and in the right and left bottom corners are well resolved. Right: The arrows show direction and modulus of interpolated velocities on a coarse raster.

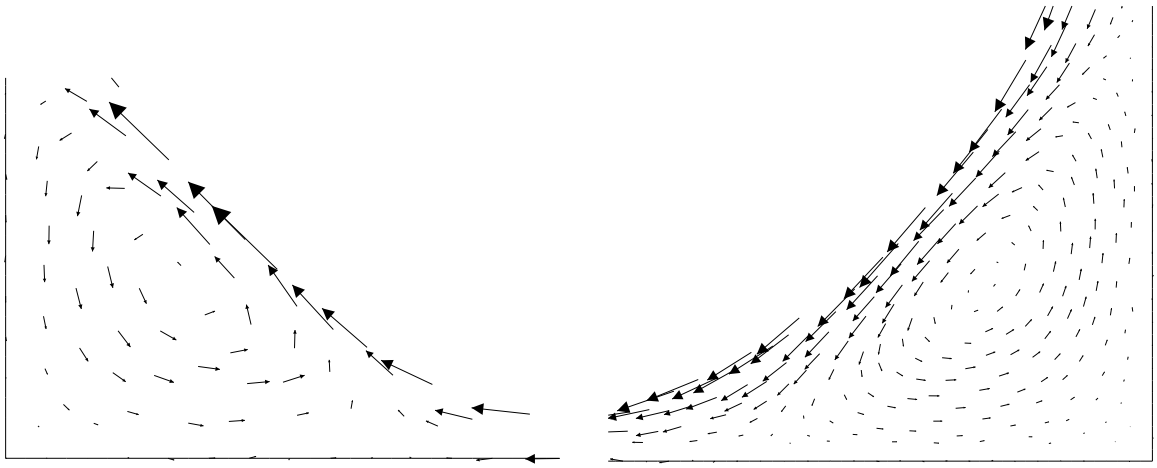

FIGURE 7. Driven cavity in a square, Reynolds number 400. The arrows show direction and modulus of interpolated velocities at vertices of the mesh. Left: Zoom into the vortex in the left bottom corner. Right: Zoom into the vortex in the right bottom corner.

classical MAC scheme as they cannot be approximated exactly by rectangular elements. We use the right hand side $\boldsymbol{f} = \mathbf{0}$. At the top of the cavity, we prescribe the velocity $\boldsymbol{v} = (0, 1)^T$. At the rest of the boundary we assume no-slip boundary conditions $\boldsymbol{v} = \mathbf{0}$. We solve the problem for the rather moderate Reynolds number 100, [**3**]. On an unstructured Delaunay grid generated by TRIANGLE [**24**] with 7,000 vertices, we needed 83 Picard iterations in order to reduce the size of the nonlinear residual to that of the direct solver PARDISO [**22, 23**]. We recover the classical results for this problem [**3**]. We find three vortices, a large one in the upper part of the cavity, and two smaller ones in the bottom part of the cavity, see Figures 8 and 9.

References

[1] Michael A. Case, Vincent J. Ervin, Alexander Linke, Leo G. Rebholz, and Nicholas E. Wilson. Stable computing with an enhanced physics based scheme for the 3D Navier-Stokes equations. *Int. J. Numer. Anal. Model.*, 8(1):118–136, 2011.

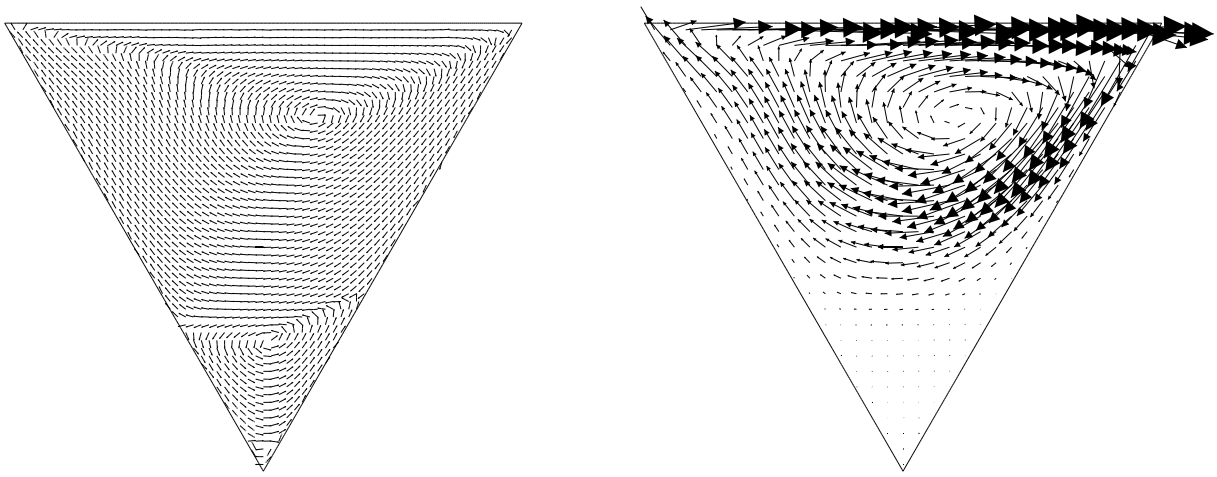

FIGURE 8. Driven cavity in an equilateral triangle, Reynolds number 100. Left: The equal length arrows show interpolated velocity directions on a coarse raster.The three vortices in the triangular cavity are resolved. Right: The arrows show direction and modulus of interpolated velocities on a coarse raster

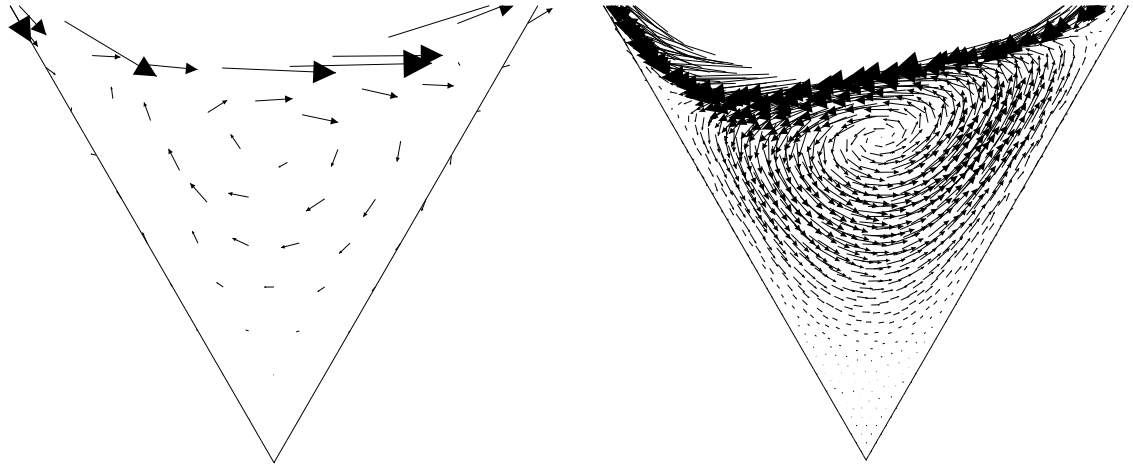

FIGURE 9. Driven cavity in an equilateral triangle, Reynolds number 100. The arrows show direction and modulus of interpolated velocities at vertices of the mesh. Left: Zoom into the small vortex at the bottom of the cavity. Right: Zoom into the medium size vortex below the dominant central vortex.

[2] J. C. Cavendish, C. A. Hall, and T. A. Porsching. Solution of incompressible Navier-Stokes equations on unstructured grids using dual tesselations. *Int. J. Num. Meth. Heat Flow*, 2:483–502, 1992.

[3] E. Erturk and O. Gokcol. Fine grid numerical solutions of triangular cavity flow. *Eur. Phys. J. Appl. Phys.*, 38(1):97–105, 2007.

[4] R. Eymard, T. Gallouët, and R. Herbin. Finite volume methods. In P. G. Ciarlet and J. L. Lions, editors, *Handbook of Numerical Analysis*, volume VII, pages 713–1020. North Holland, 2000.

[5] R. Eymard, T. Gallouët, and R. Herbin. A cell-centered finite-volume approximation for anisotropic diffusion operators on unstructured meshes in any space dimension. *IMA J. Numer. Anal.*, 26(2):326–353, 2006.

[6] R. Eymard, T. Gallouët, R. Herbin, and A. Linke. Finite volume schemes for the biharmonic problem on general meshes. *Math. Comp.*, accepted for publication, 2011.

[7] R. Eymard, R. Herbin, and M. Rhoudaf. Approximation of the biharmonic problem using P_1 finite elements. *J. of Num. Math.*, 19(1):1–26, 2011.

[8] J. Fuhrmann et al. Pdelib. www.wias-berlin.de/software/pdelib/.

[9] J. Fuhrmann, H. Langmach, and A. Linke. A numerical method for mass conservative coupling between fluid flow and solute transport. *Applied Numerical Mathematics*, 61(4):530–553, 2011.

[10] J. Fuhrmann, A. Linke, H. Langmach, and H. Baltruschat. Numerical calculation of the limiting current for a cylindrical thin layer flow cell. *Electrochimica Acta*, 55(2):430–438, 2009.

[11] U. Ghia, K. N. Ghia, and C. T. Shin. High-Resolutions for incompressible flow using the Navier-Stokes equations and a multigrid method. *J. Comput. Phys.*, 48:387–411, 1982.

[12] W. Hackbusch. On first and second order box schemes. *Computing*, 41(4):277–296, 1989.

[13] C. A. Hall, J. C. Cavendish, and W. H. Frey. The dual variable method for solving fluid flow difference equations on Delaunay triangulations. *Comput. & Fluids*, 20(2):145–164, 1991.

[14] C. A. Hall and T. A. Porsching. A characteristic-like method for thermally expandable flow on unstructured triangular grids. *Internat. J. Numer. Methods Fluids*, 22(8):731–754, 1996.

[15] F. H. Harlow and J. E. Welch. Numerical calculation of time-dependent viscous incompressible flow of fluid with free surface. *Physics of fluids*, 8(12):2182–2189, 1965.

[16] Guido Kanschat. Divergence-free discontinuous Galerkin schemes for the Stokes equations and the MAC scheme. *Internat. J. Numer. Methods Fluids*, 56(7):941–950, 2008.

[17] J. Nicolaides, T. A. Porsching, and C. A. Hall. Covolume methods in computational fluid dynamics. In M. Hafez and K. Oshma, editors, *Computation Fluid Dynamics Review*, pages 279–299. John Wiley and Sons, New York, 1995.

[18] R. A. Nicolaides. Analysis and convergence of the MAC scheme. I. The linear problem. *SIAM J. Numer. Anal.*, 29(6):1579–1591, 1992.

[19] R. A. Nicolaides and X. Wu. Analysis and convergence of the MAC scheme. II. Navier-Stokes equations. *Math. Comp.*, 65(213):29–44, 1996.

[20] R.A. Nicolaides. *Incompressible Computational Fluid Dynamics*. M.D Gunzburger and R.A. Nicolaides (Cambridge Univ.Press, Cambridge, U.K), 1993.

[21] S. V. Patankar. Numerical heat transfer and fluid flow. *Series in Computational Methods in Mechanics and Thermal Sciences, Minkowycz and Sparrow Eds.*, 1980.

[22] O. Schenk, K. Gärtner, and W. Fichtner. Efficient sparse LU factorization with left-right looking strategy on shared memory multiprocessors. *BIT*, 40(1):158–176, 1999.

[23] O. Schenk, K. Gärtner, G. Karypis, S. Röllin, and M. Hagemann. PARDISO Solver Project. URL: http://www.pardiso-project.org, 2011. Retrieved 2011-09-20.

[24] J. R. Shewchuk. triangle version 1.6.
URL: http://www.cs.cmu.edu/˜quake/triangle.html, 2005. Retrieved 2011-09-20.

[25] H. Si, K. Gärtner, and J. Fuhrmann. Boundary conforming Delaunay mesh generation. *Comput. Math. Math. Phys.*, 50:38–53, 2010.

[26] R. Temam. *Navier-Stokes equations*. Elsevier, North-Holland, 1991.